Domain wall configurations in multilayered rings

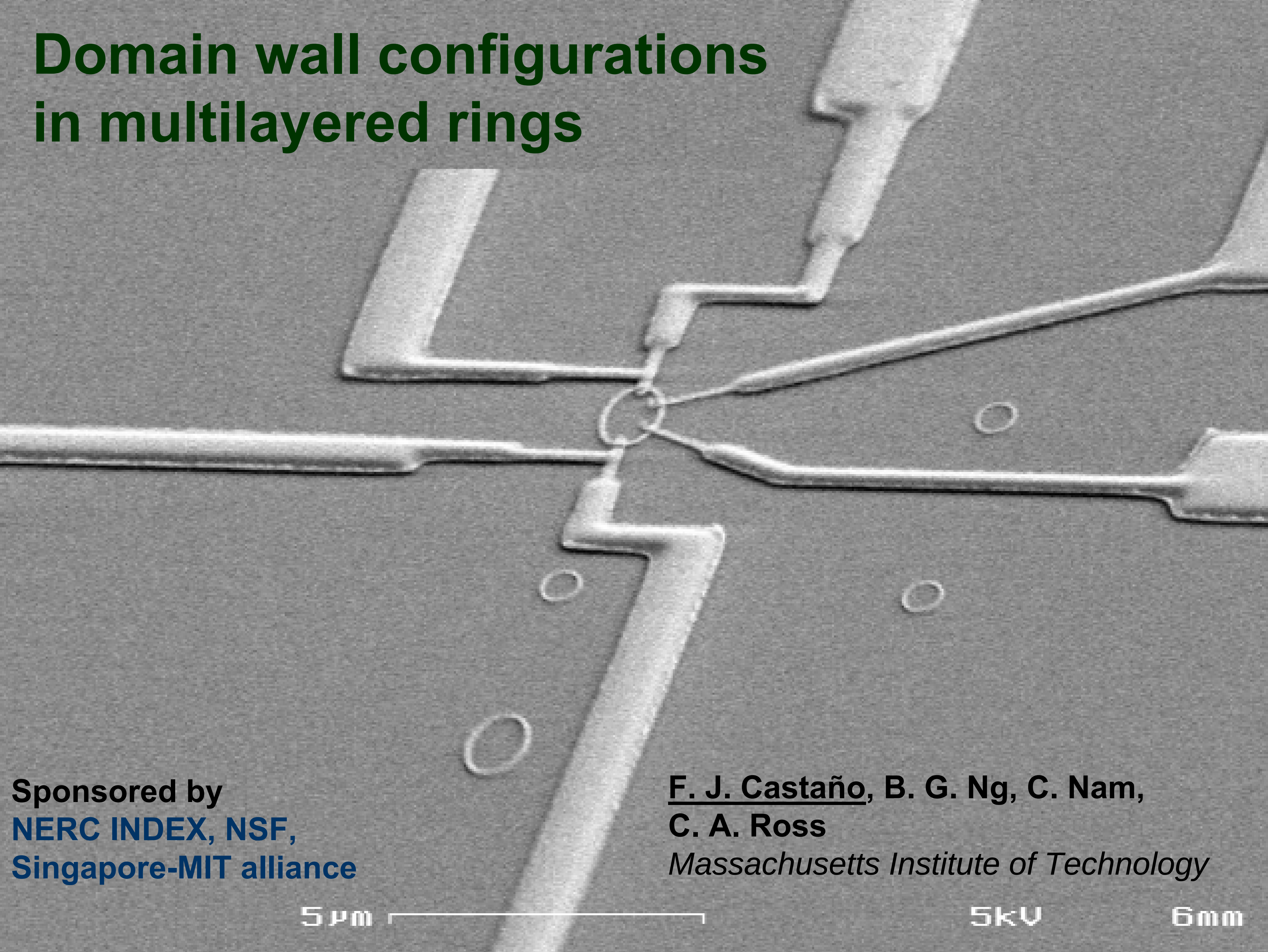

Sponsored by
NERC INDEX, NSF, Singapore-MIT alliance

F. J. Castaño, B. G. Ng, C. Nam, C. A. Ross
Massachusetts Institute of Technology

Outline

- Introduction
- NiFe/Cu/Co and NiFe/Cu/Co/IrMn elliptical and rhombic rings
- Magneto-resistance response
  - 4-point measurements
  - Wheatstone bridge configuration
- Micromagnetic modeling
- Current-induced switching
- Multi-bit storage and logic operation
- Summary

Introduction. MRAMs

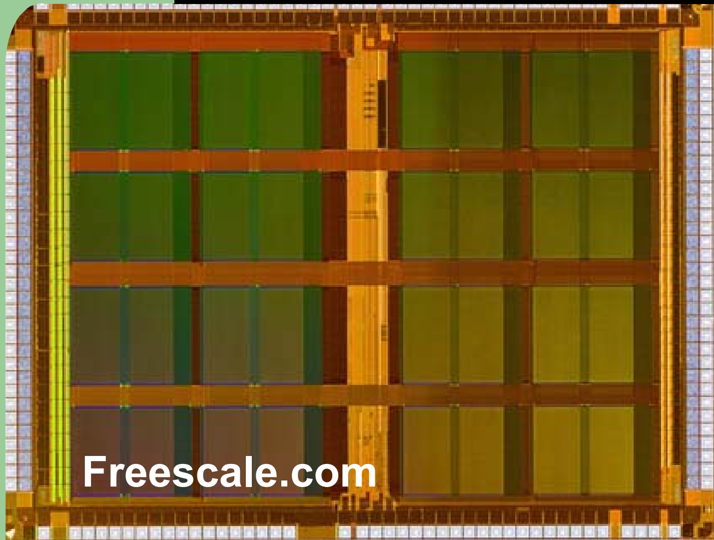

- **Magnetic Random Access Memories.**

  Field-induced write

  Freescale (2006). MR2A16A-4Mb 1T/1MTJ 3.3V memory on 0.18µm CMOS, 35ns access time, ~10 mA write current. 1.5 µm² cell size, MTJ.

  Current-induced write.

  Hitachi (2008). 2Mb 1T/1MTJ 1.8V memory on 0.18µm CMOS, 40ns access time, ~200 µ A write current. 1.6 x 1.6 µm² cell size.

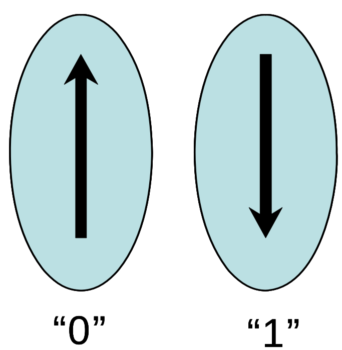

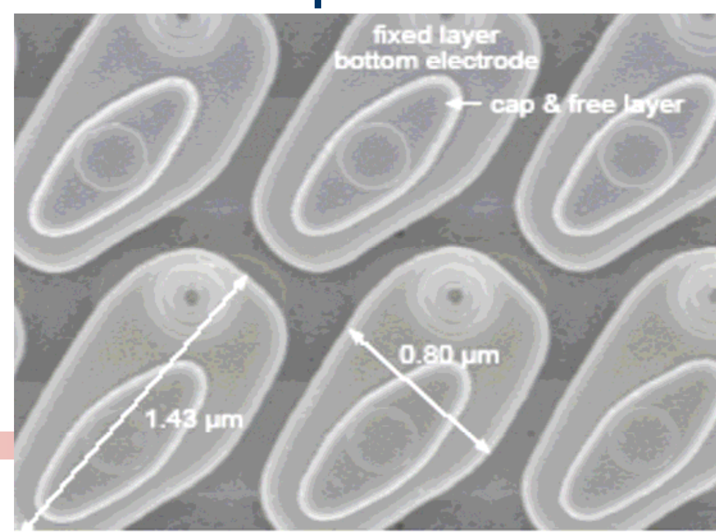

Introduction. Single-layer magnetic rings

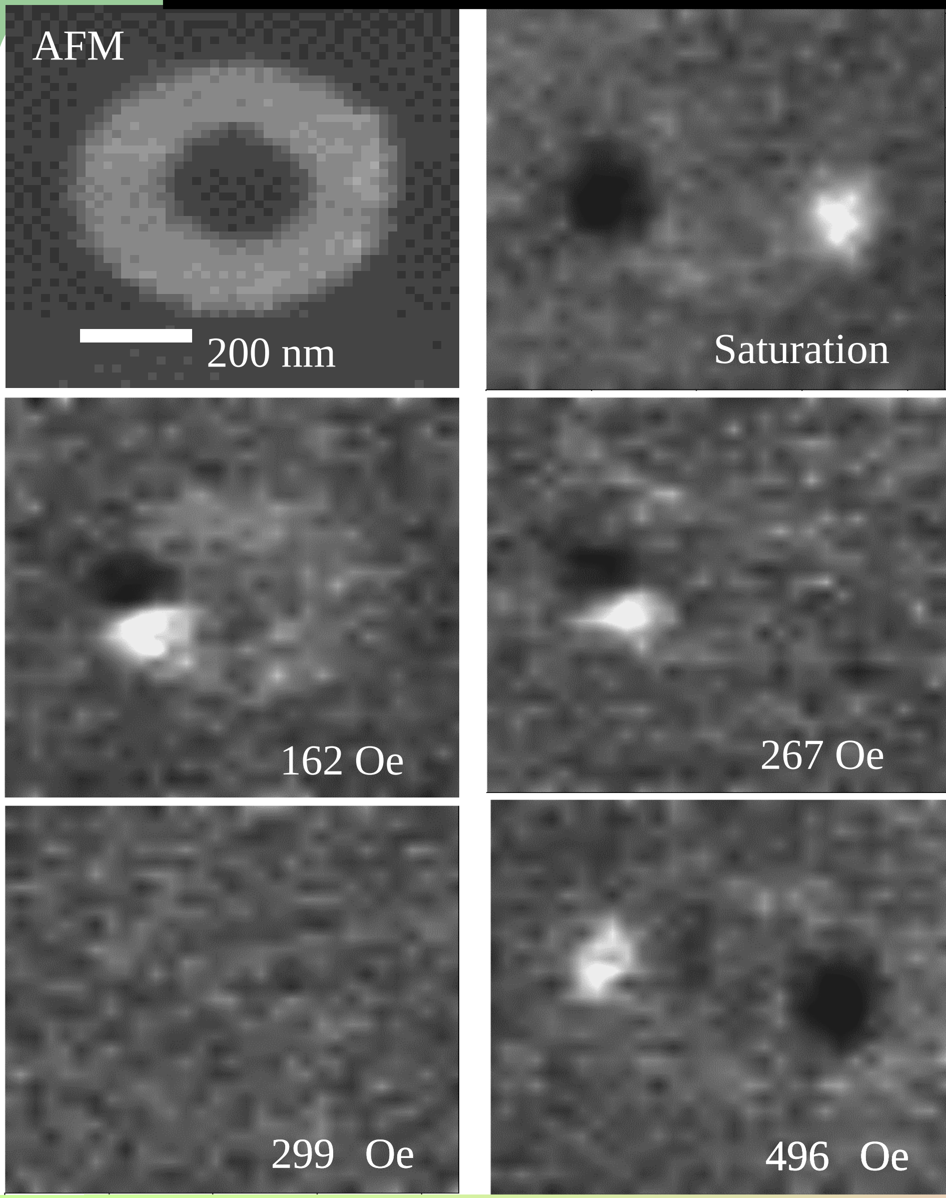

- As an alternative bit shape, magnetic rings are interesting because of the existence multiple stable and metastable states.
- 360˚ wall.

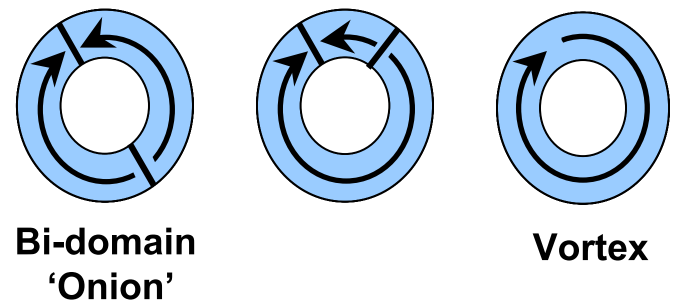

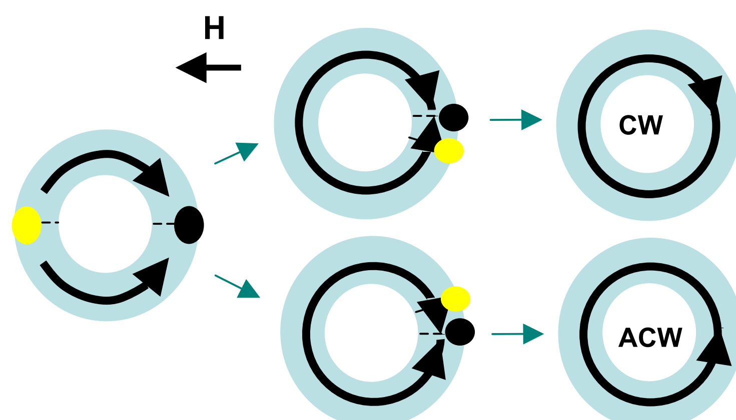

Introduction. Magnetic rings

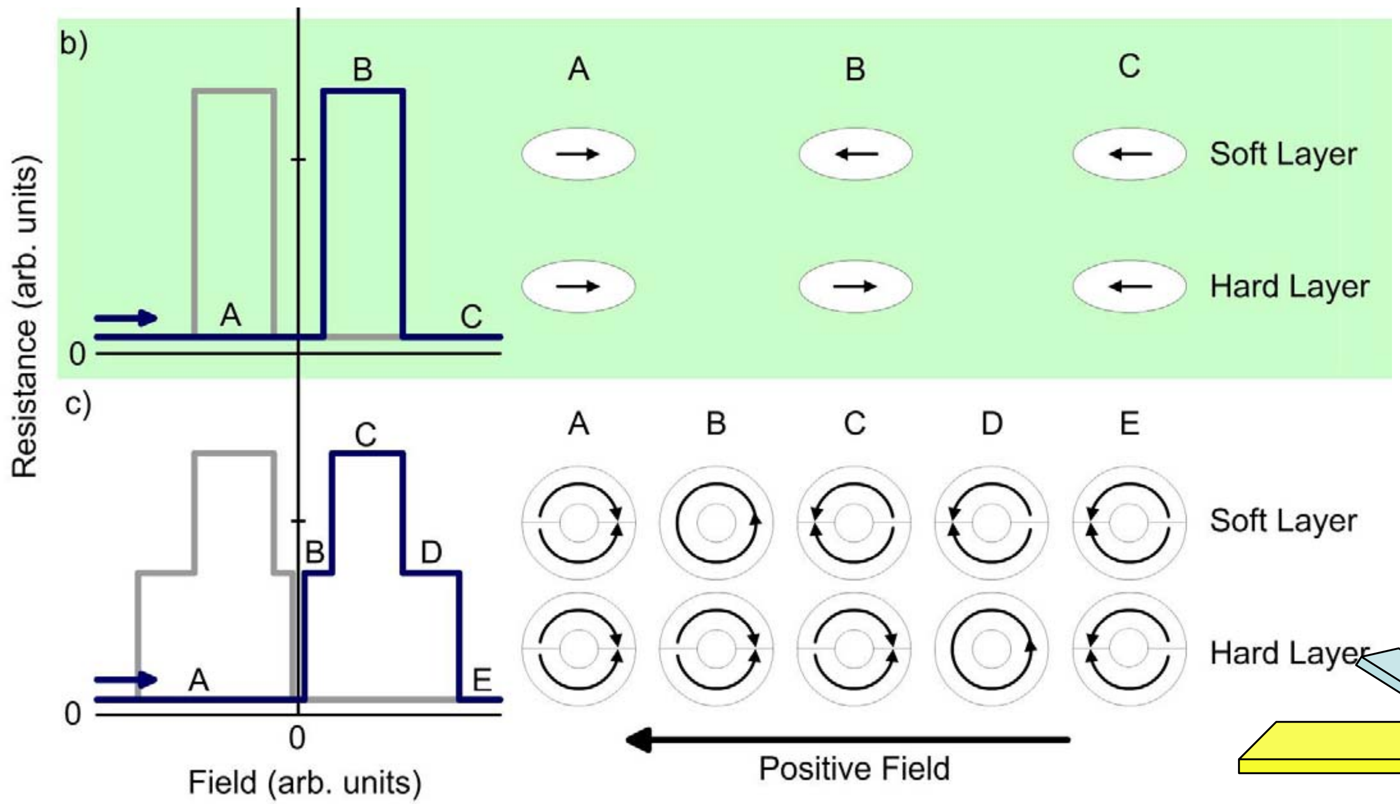

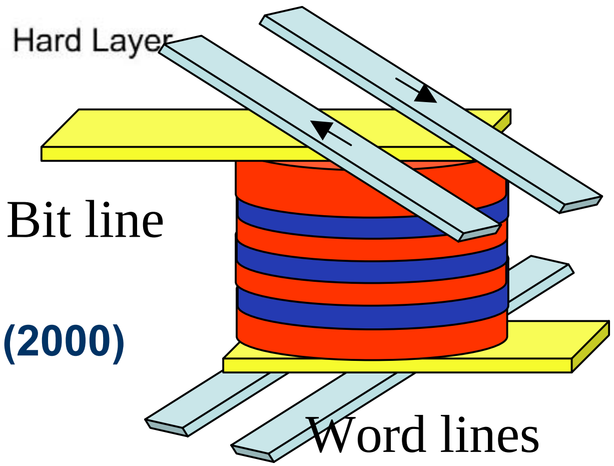

Zhu et al, J. Appl. Phys. 87 6668 (2000)

Multilayered elliptical and rhombic ring devices

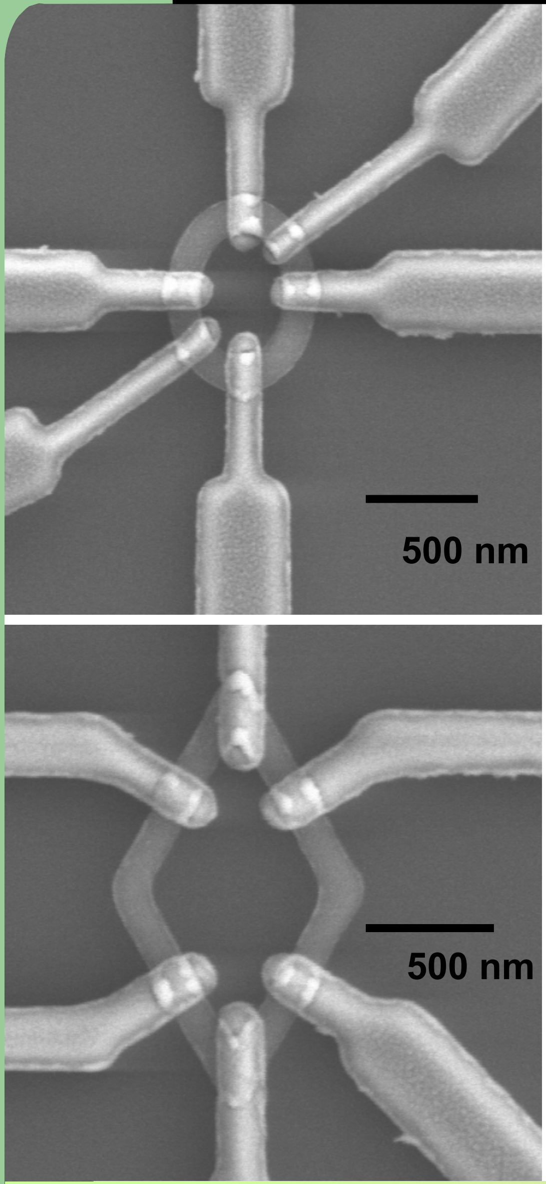

- Shape anisotropy. Controlled positioning of domain walls.
- Elliptical and rhombic layered rings.
  NiFe/Cu/Co (Pseudo-spin-valve)
  NiFe/Cu/Co/IrMn (Spin-valve)
- Fabricated Devices. Long axis 900nm-5μm
  Widths 80nm-350nm
  Modest GMR up to 3.5%
- Magneto-transport response using an in-plane magnetic fields and different contact configurations.
- Micromagnetic modeling. Understand magnetization reversal and address scalability for both elliptical and rhombic rings.
  Long axis 150nm-2μm
  Widths 20nm-120nm

Magneto-resistance response

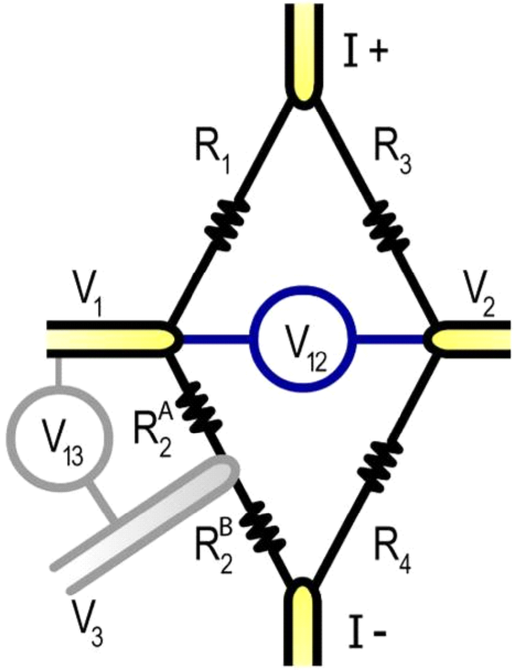

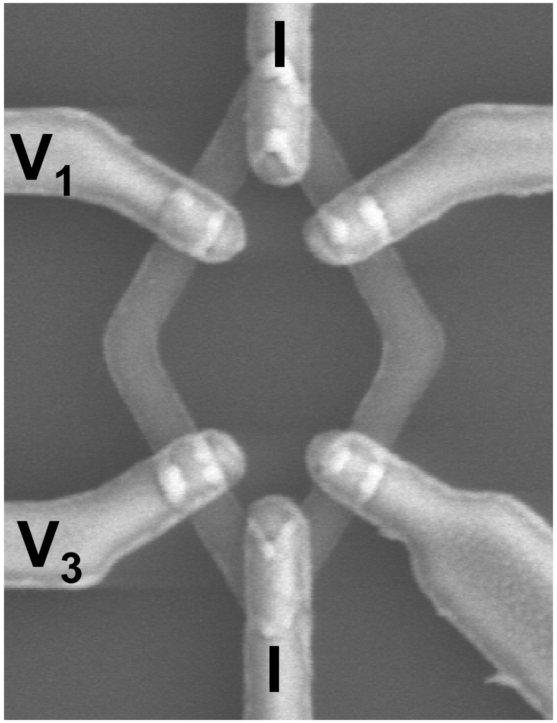

⊙ 4-point. V_{13}/I

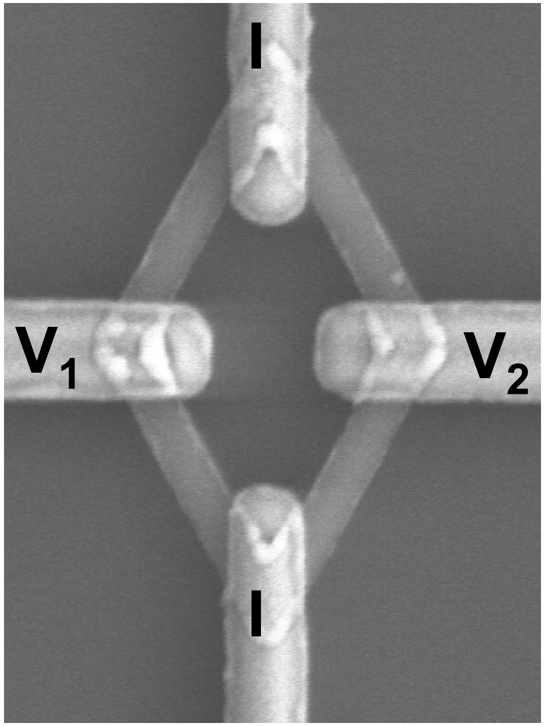

⊙ Wheatstone bridge. V_{12}/I

$$\frac{V_{13}}{I} = \frac{R_2{}^A}{R_1 + R_2^A + R_2^B} V_S + C$$

$$V_S = I_S \frac{(R_1 + R_2^A + R_2^B)(R_3 + R_4)}{R_1 + R_2^A + R_2^B + R_3 + R_4}$$

$$\frac{V_{12}}{I} = \left| \frac{R_4}{R_3 + R_4} - \frac{R_2^A + R_2^B}{R_1 + R_2^A + R_2^B} \right| \cdot (V_S + C)$$

⊙ WB is sensitive to small differences in resistance between the arms of the bridge.

4-point measurements. Major loops

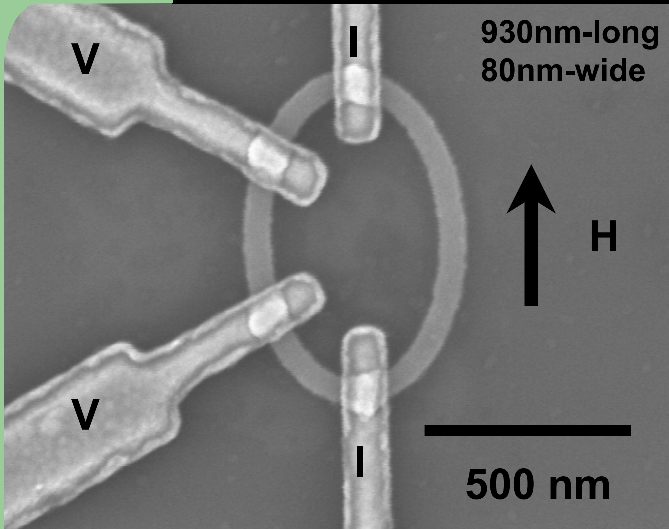

NiFe (6 nm)/Cu (4 nm)/Co (5 nm)/Au (4 nm)

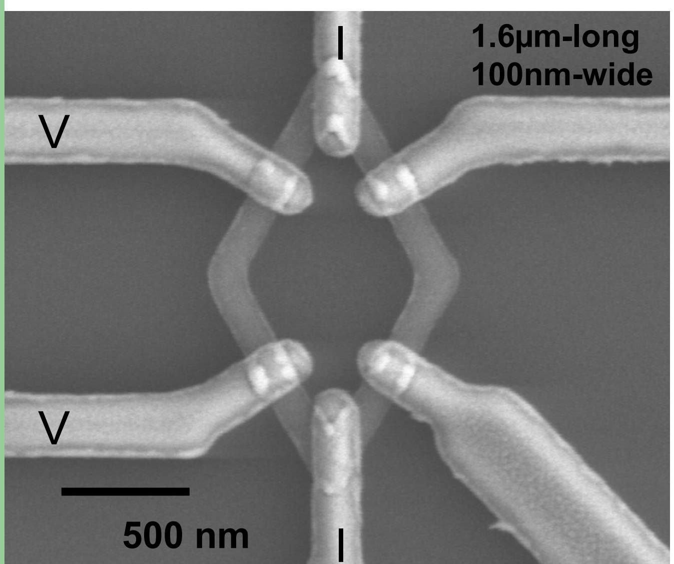

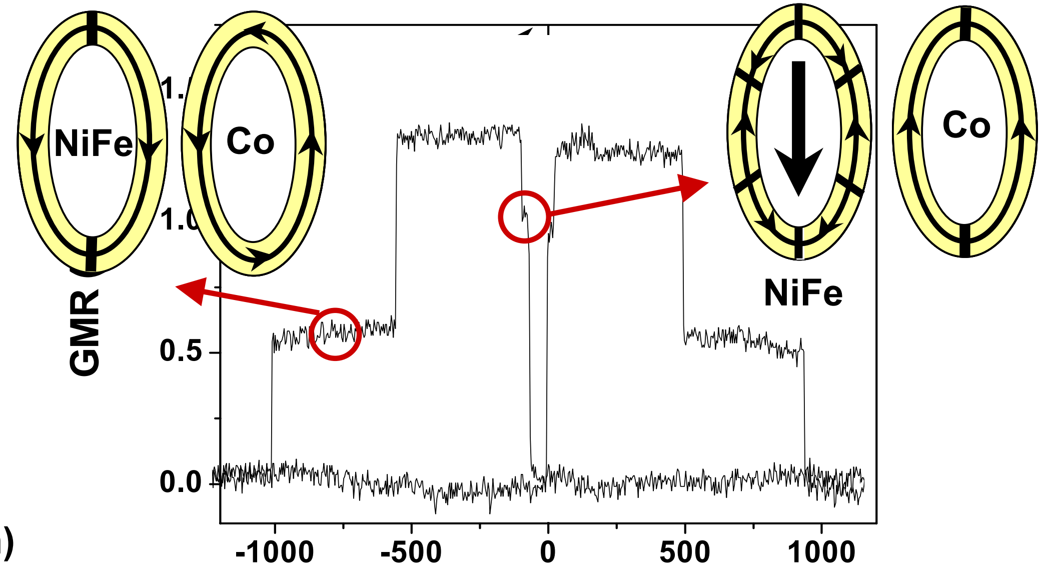

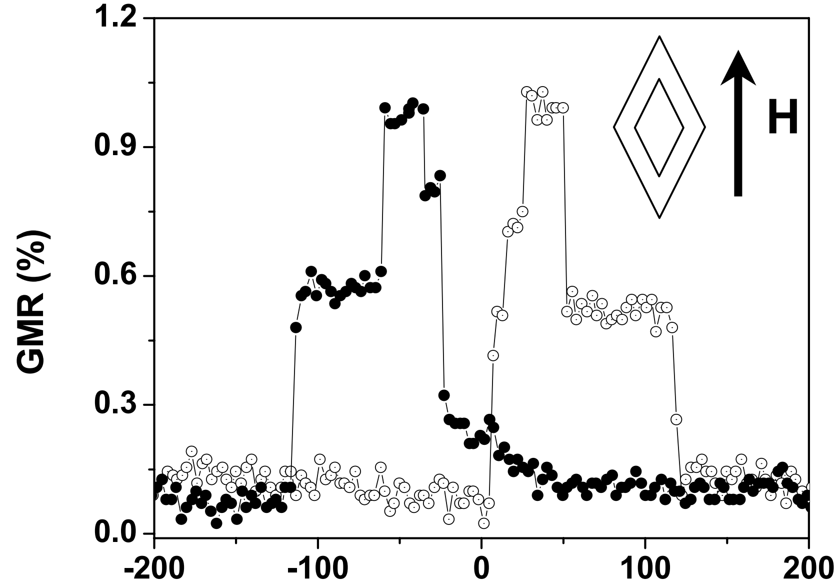

4-point measurements. Minor loops

- Cycling soft NiFe rings when Co rings are in bi-domain ('onion').
- Significant magnetostatic interactions due to the presence of domain walls in each ring.

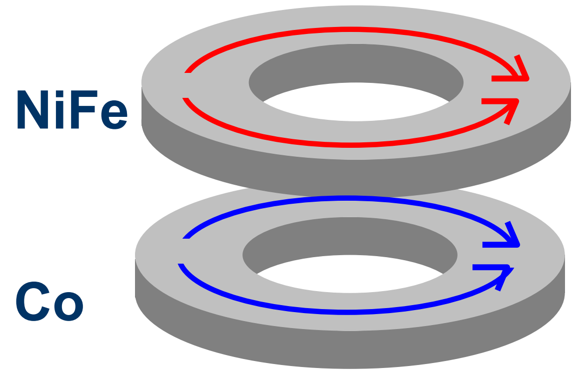

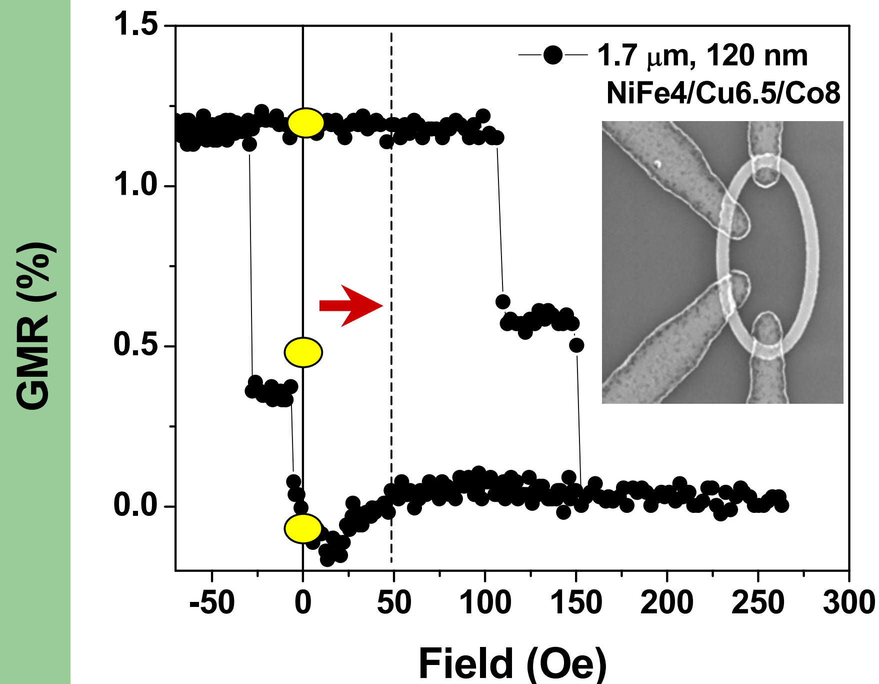

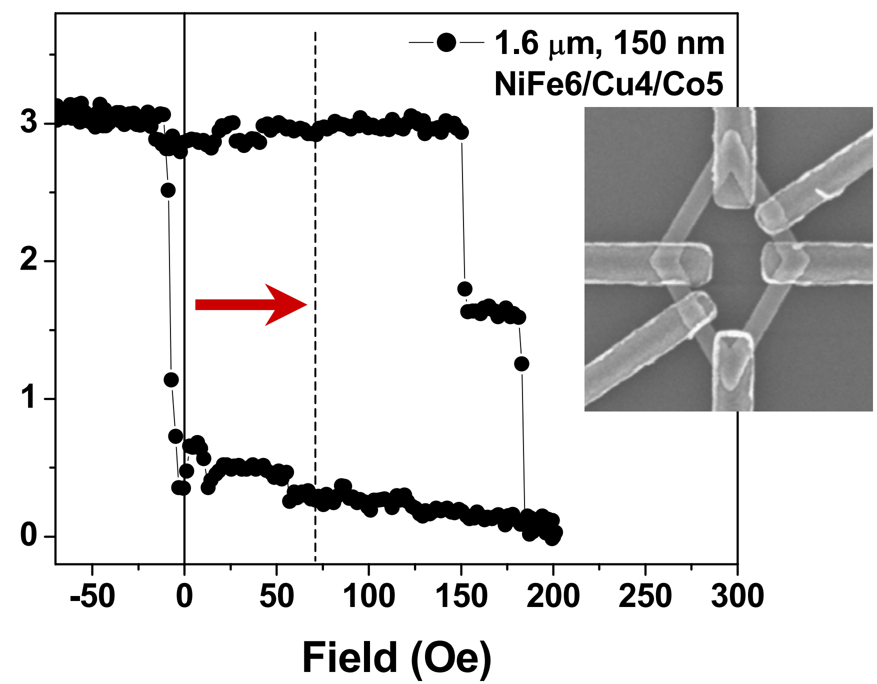

- Three distinct remanent resistance levels

4-point measurements. Minor loops

- Cycling soft NiFe rings with Co rings in a vortex configurations.
- Weak magnetostatic interactions

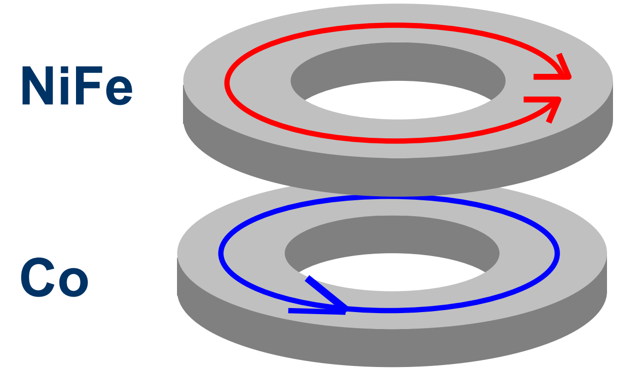

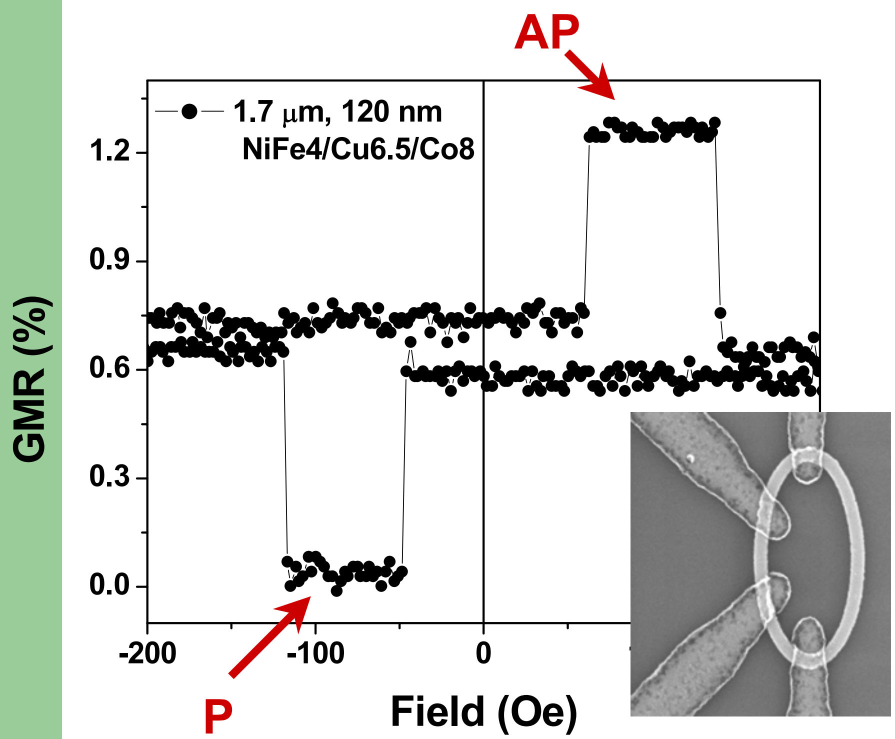

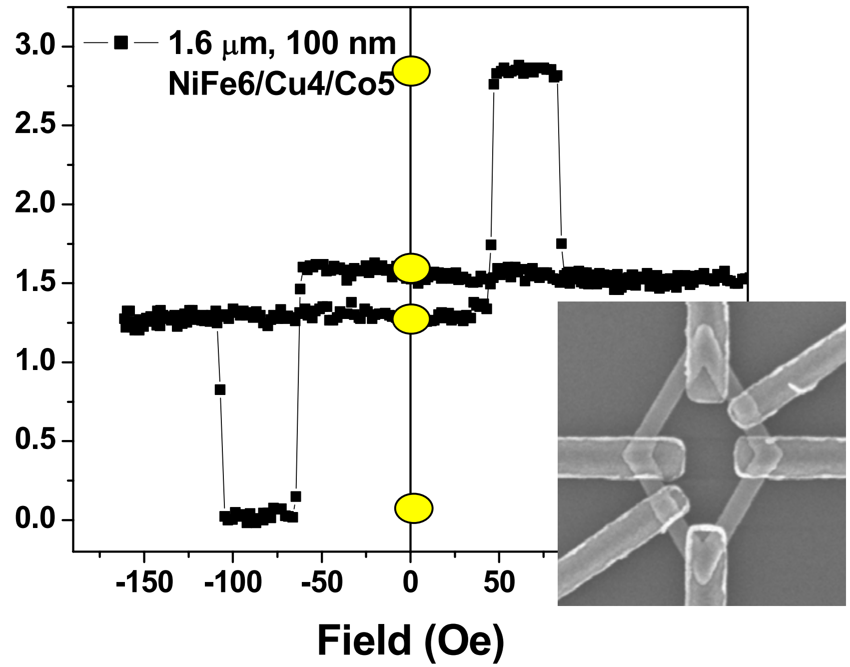

- Four distinct remanent resistance levels

4-point measurements. Spin-valve rings

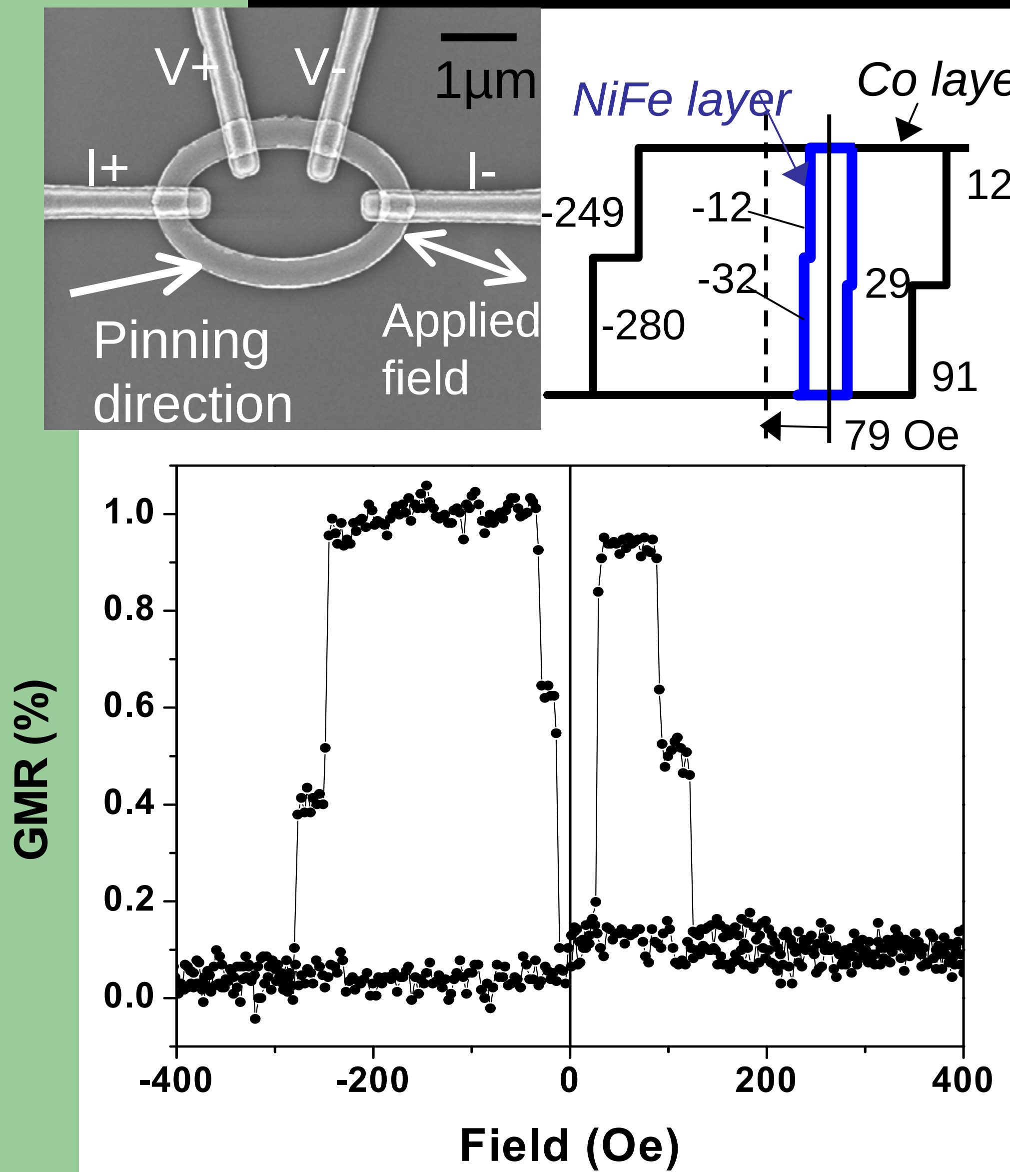

- NiFe/Cu/Co/IrMn rings
- The interplay between shape anisotropy and exchange bias allows control over the vortex chirality in the hard rings

Jung et al, PRL 2006

- Asymmetric major loops
- Minor loops (not shown) demonstrate that control of the chirality of the vortex in each ferromagnetic layer is possible, enabling at least 16 distinct magnetic configurations to be formed.
- Despite similar remanence, different configurations may be distinguished using small field perturbations.

Wheatstone Bridge. NiFe/Cu/Co elliptical rings

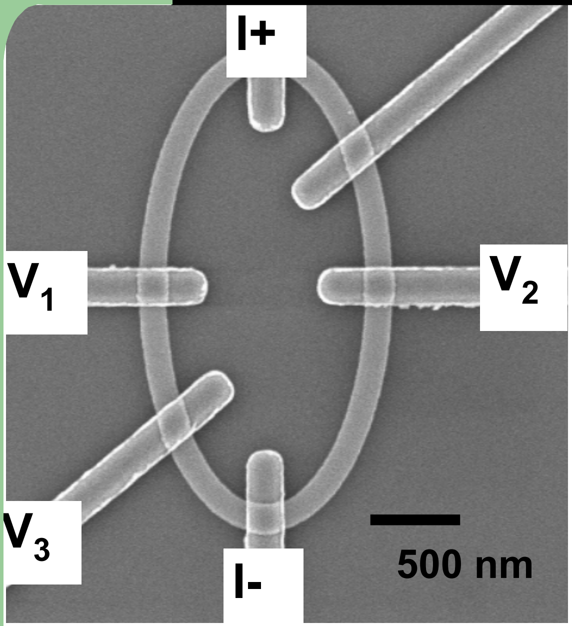

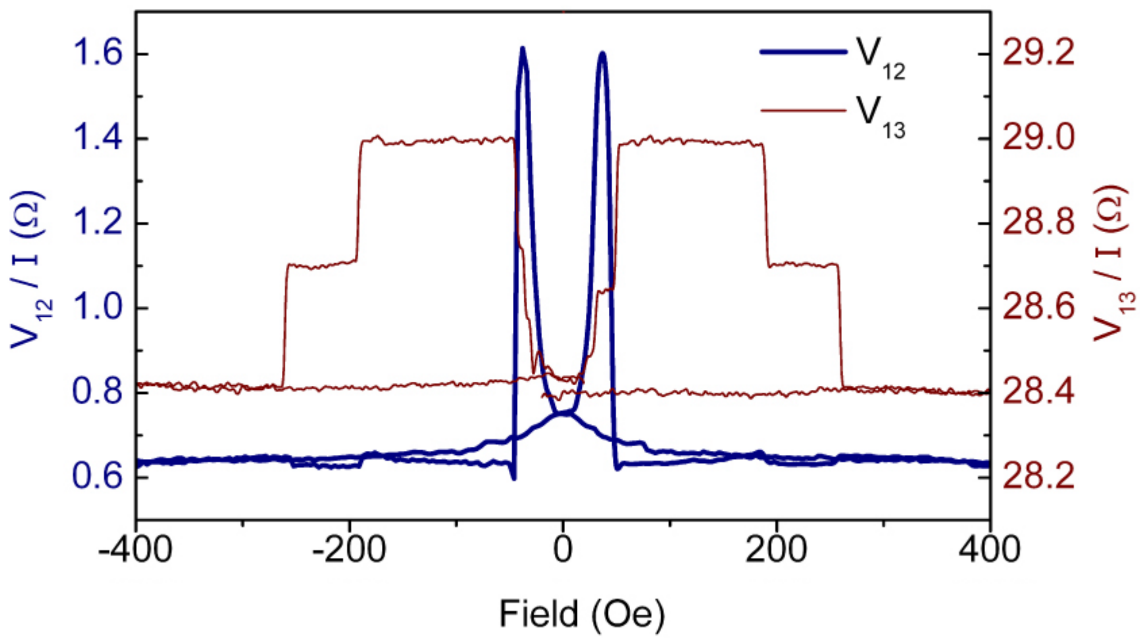

- Larger rings became unbalanced as the soft ring transitions into a vortex-like configuration.
- Three remanent configurations
- Large relative resistance changes

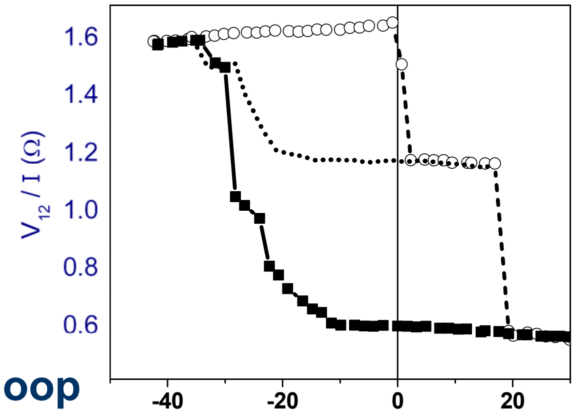

- Soft ring minor loop

Wheatstone Bridge. NiFe/Cu/Co elliptical rings

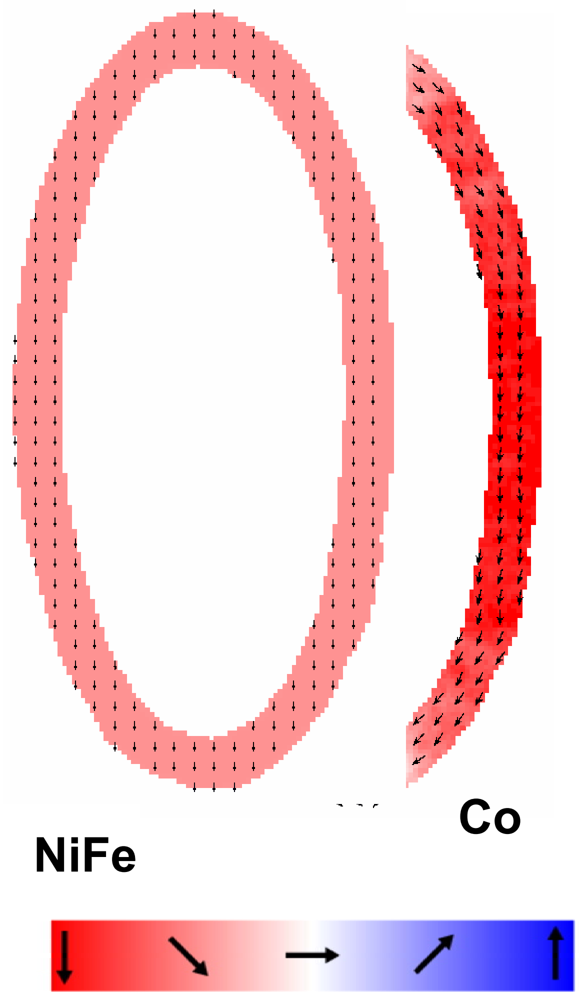

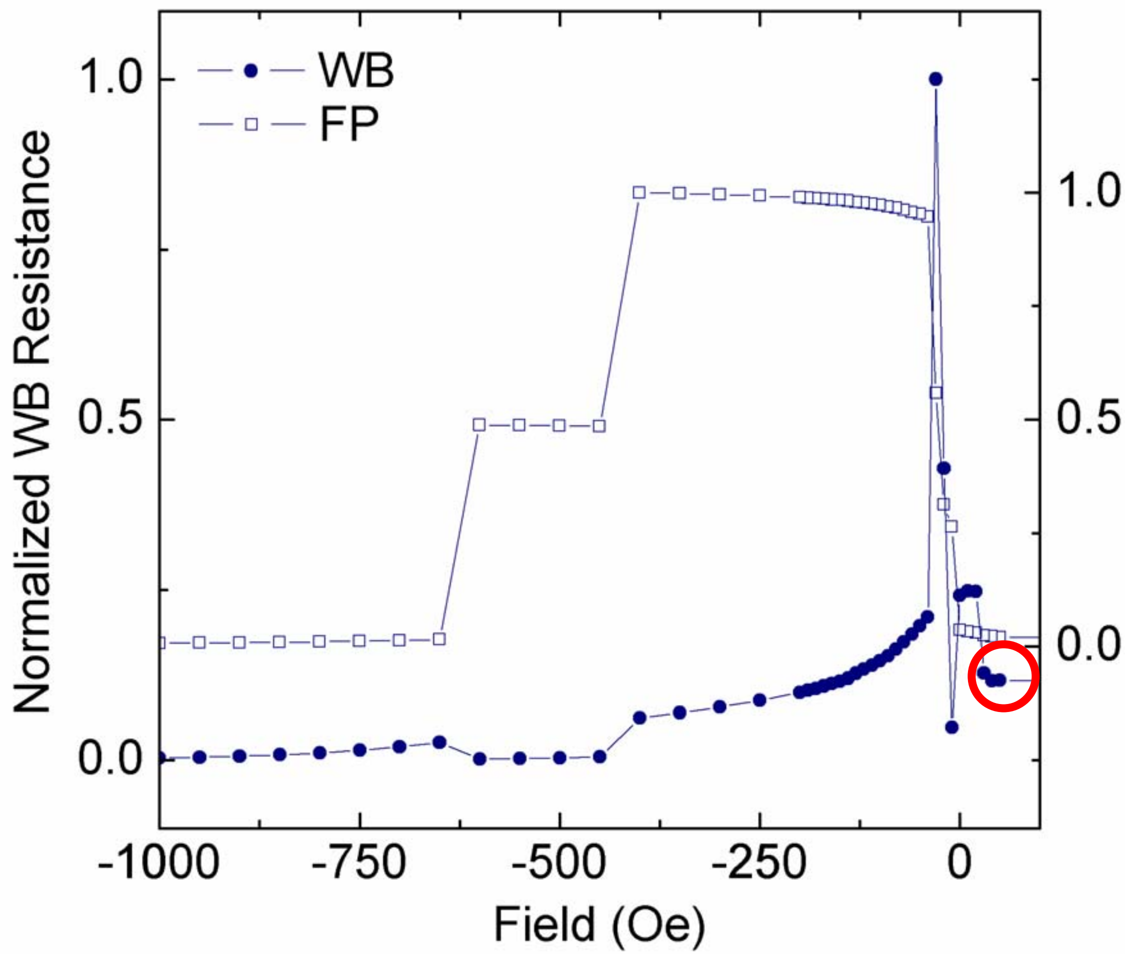

Wheatstone Bridge. NiFe/Cu/Co elliptical rings

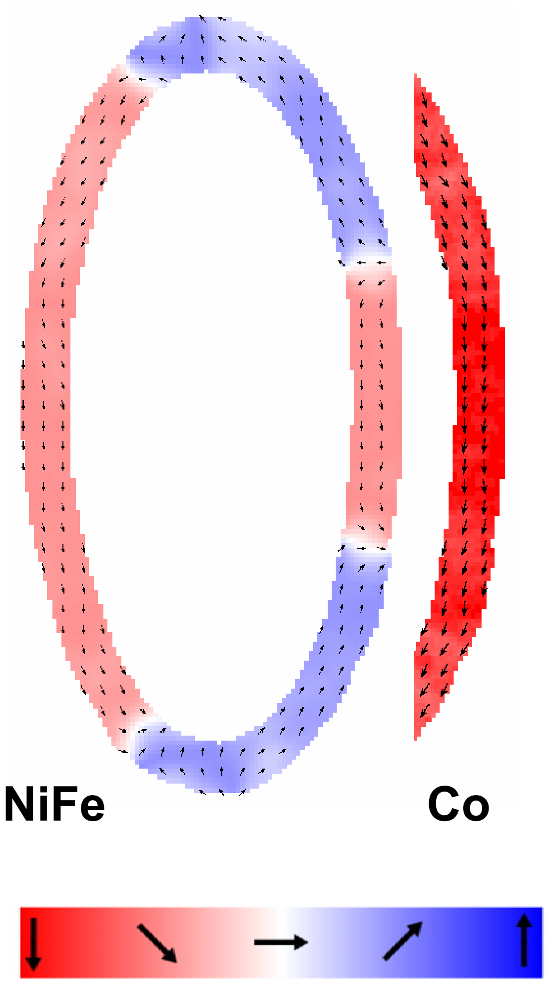

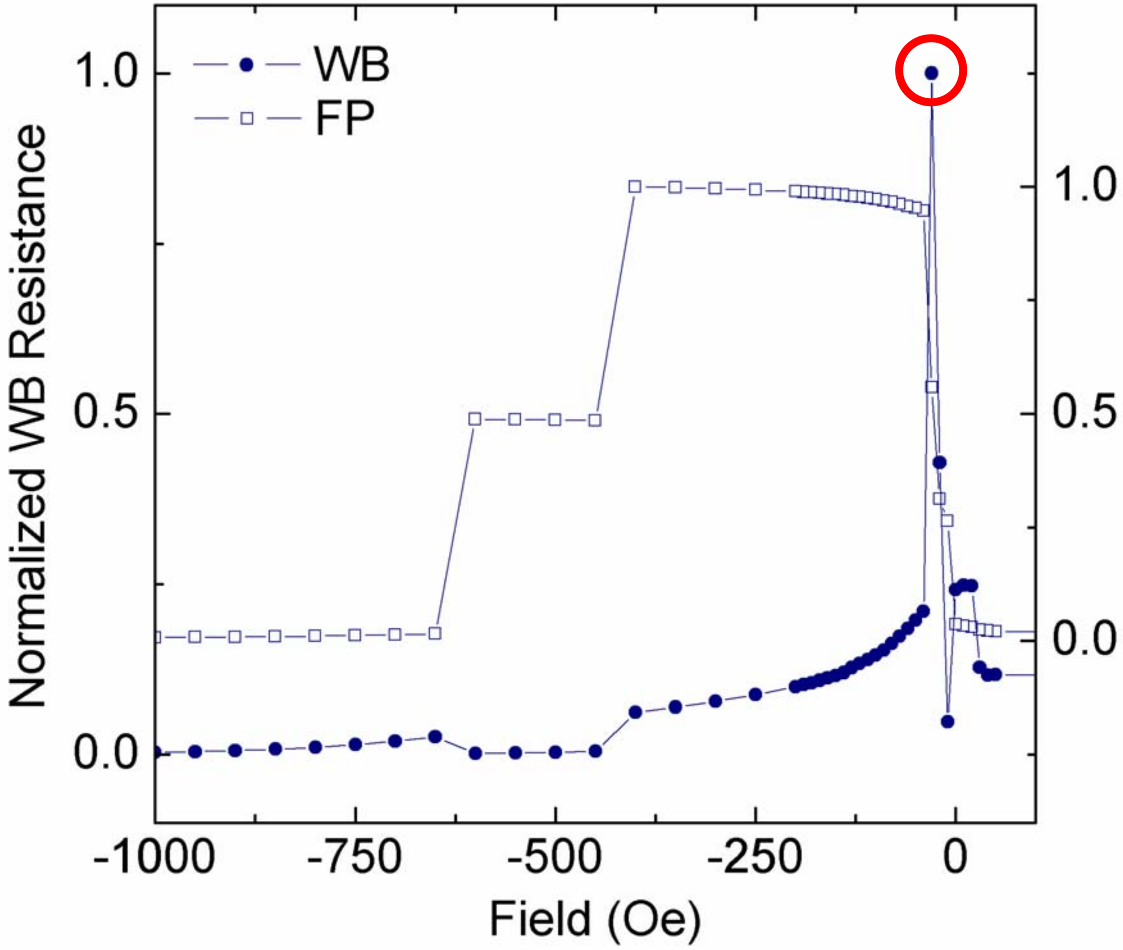

Wheatstone Bridge. NiFe/Cu/Co elliptical rings

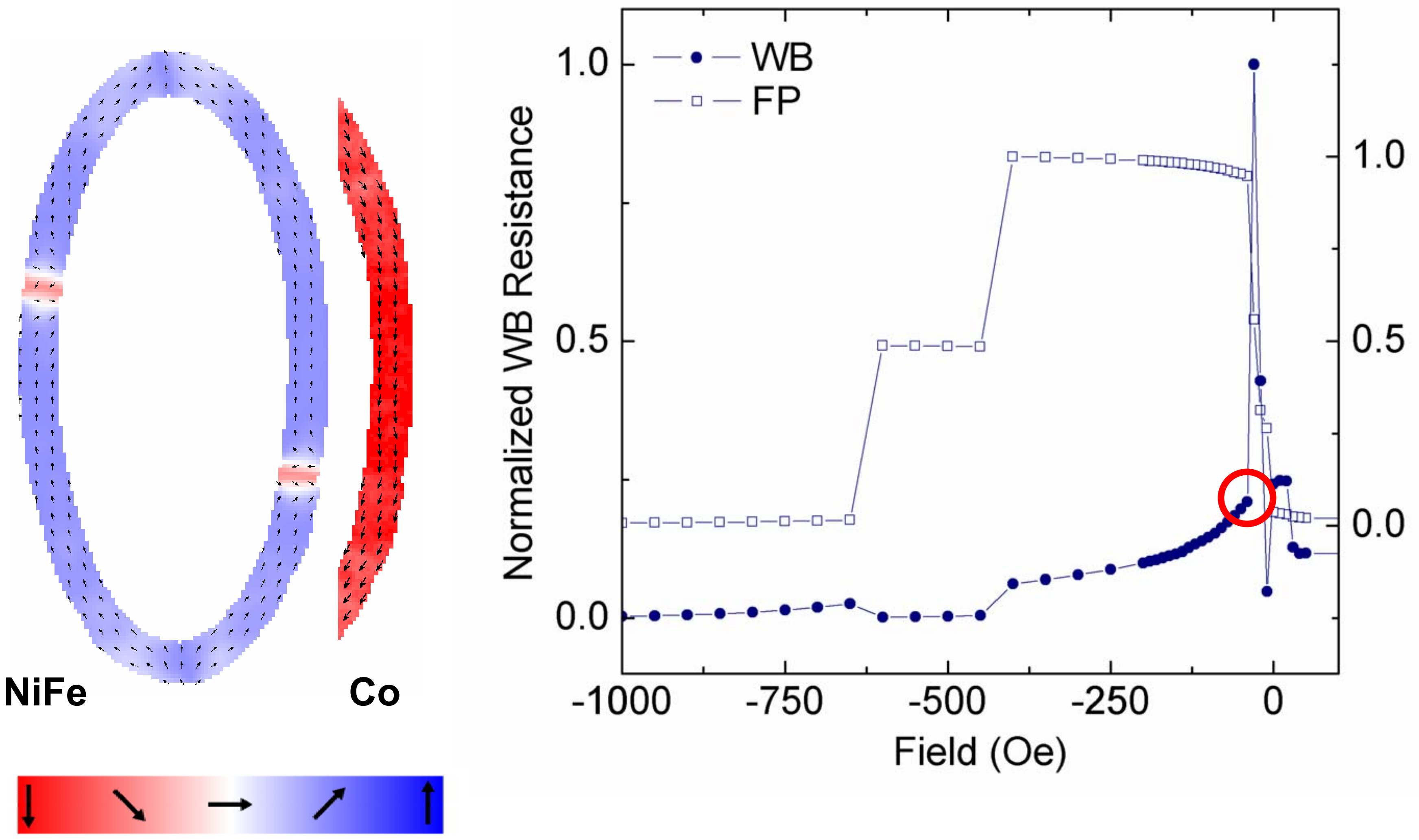

Wheatstone Bridge. NiFe/Cu/Co elliptical rings

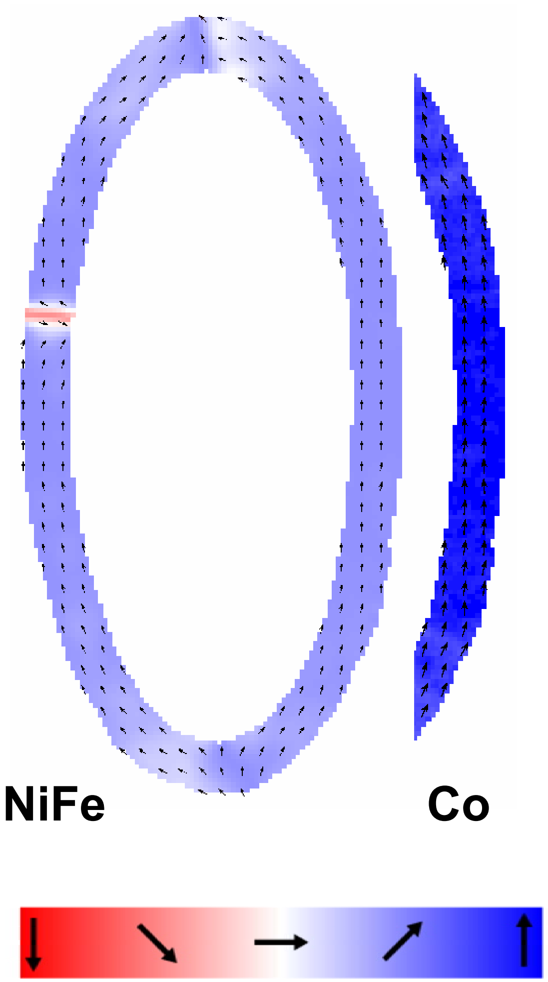

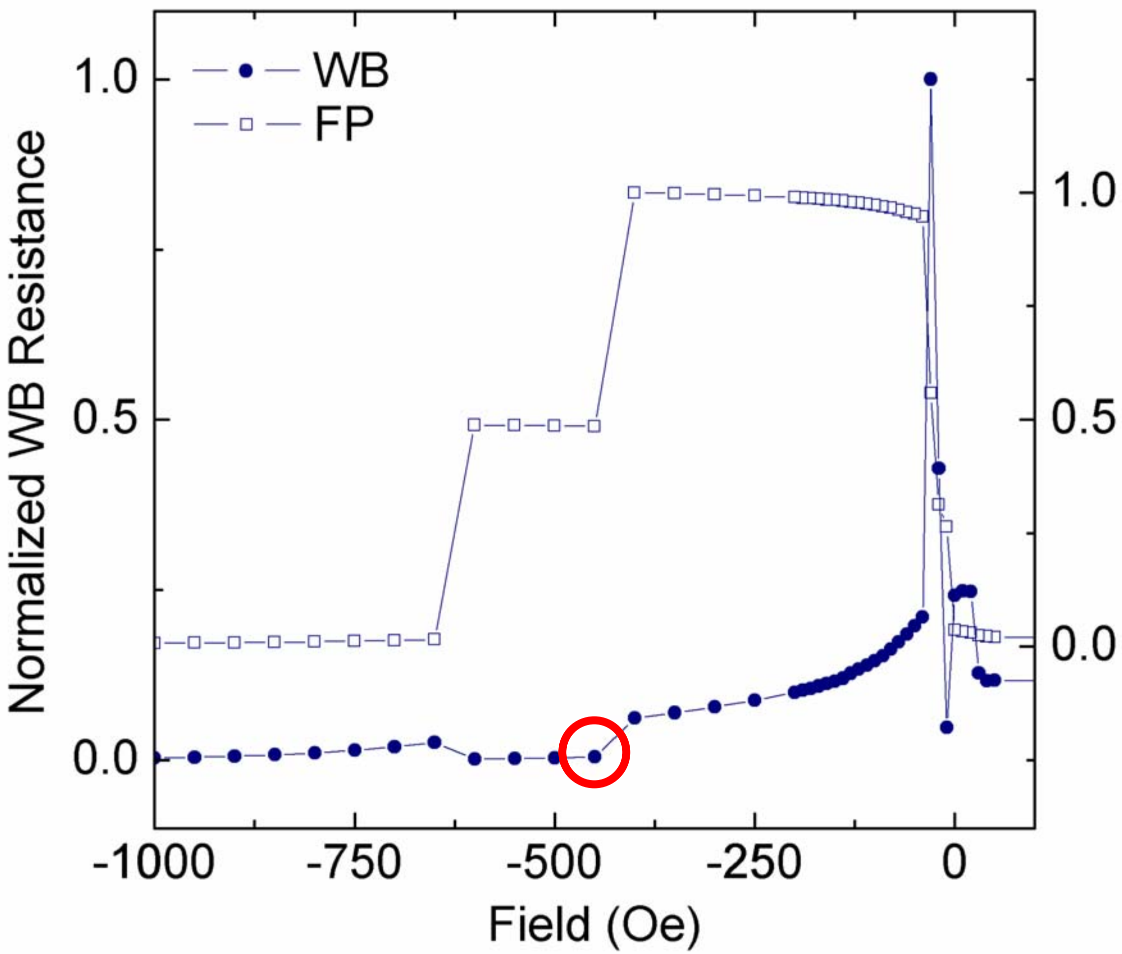

Wheatstone Bridge. NiFe/Cu/Co elliptical rings

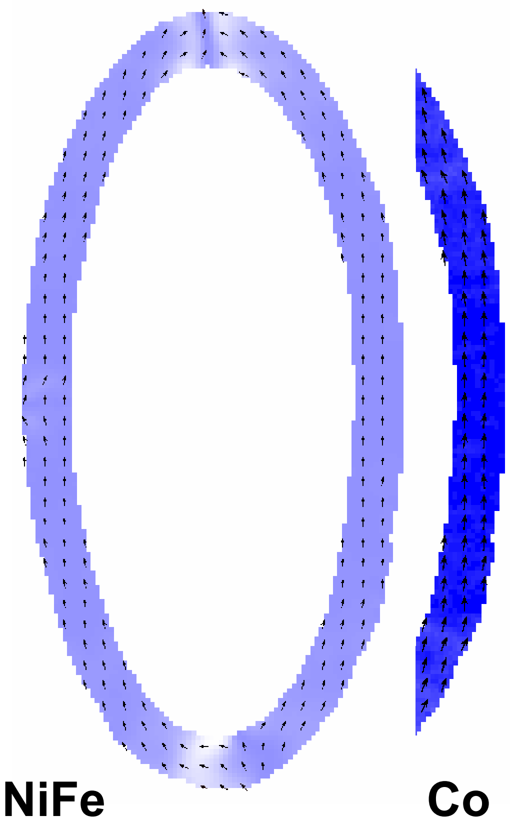

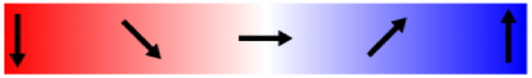

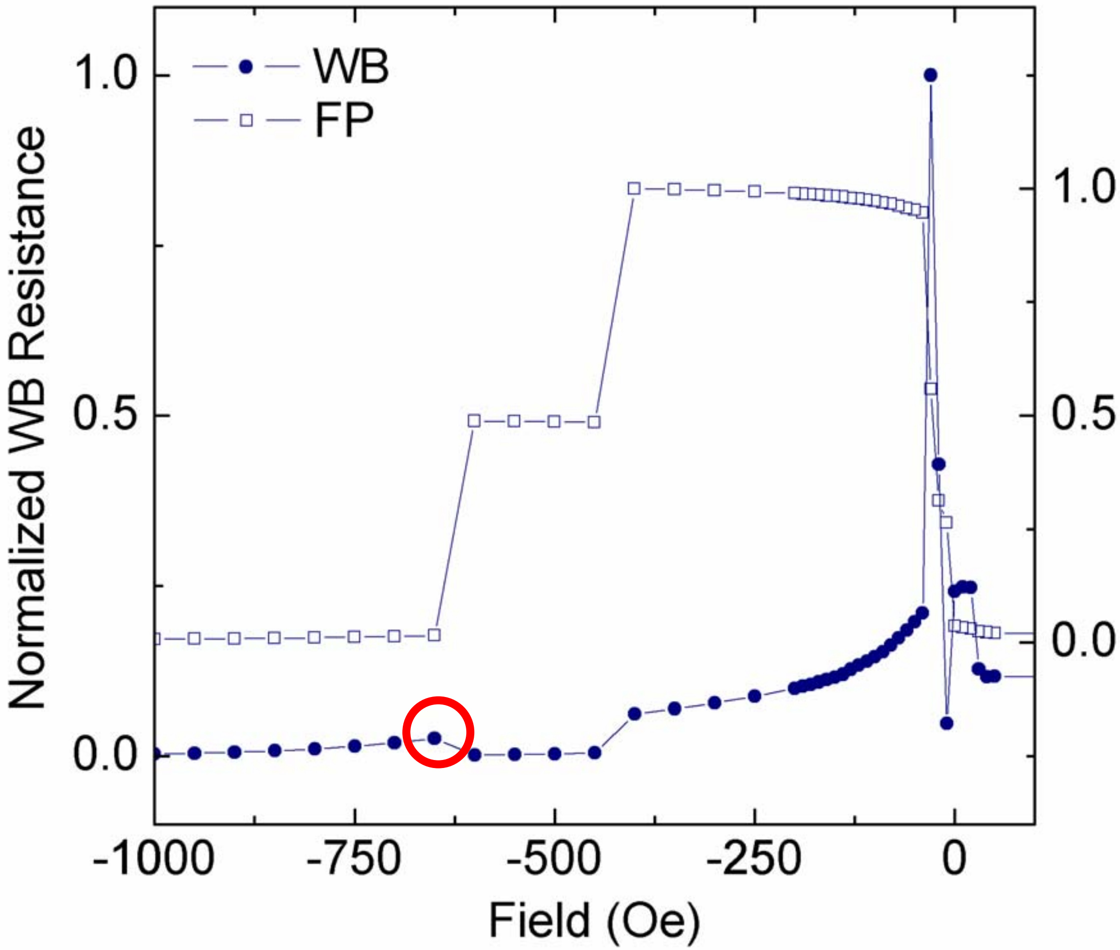

Wheatstone Bridge. NiFe/Cu/Co elliptical rings

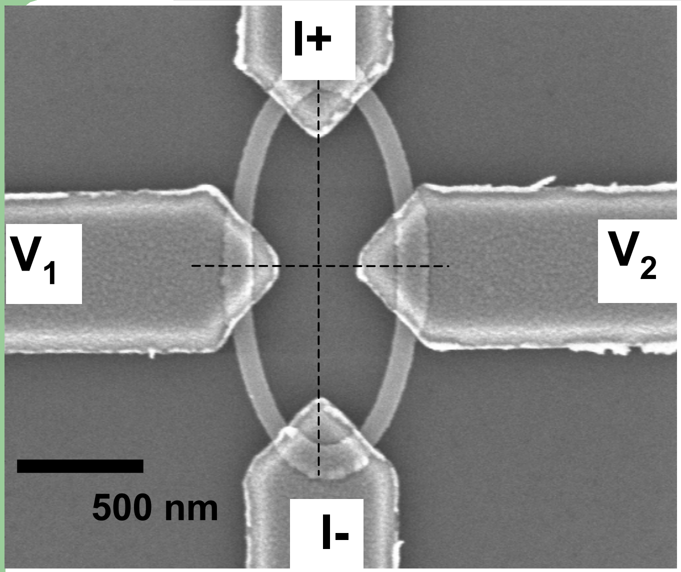

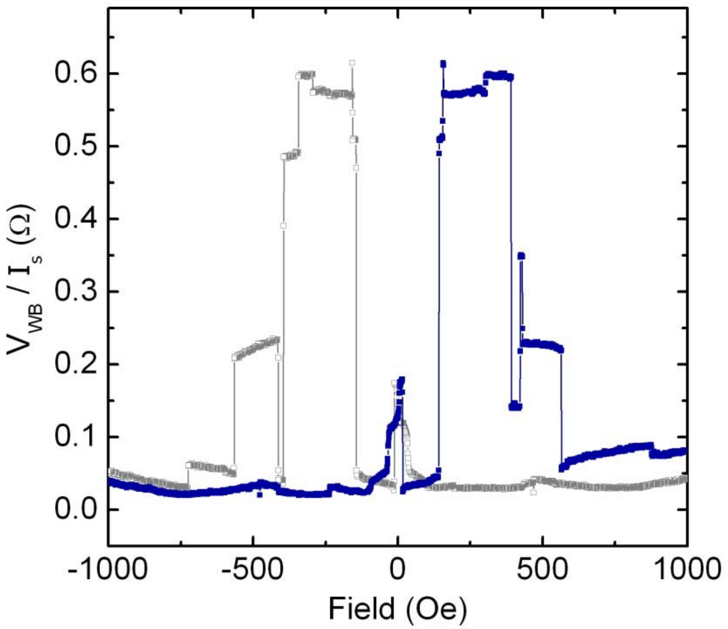

- ⊙ **Smaller/narrower rings became unbalanced as both the soft and hard rings reverse through vortex-like configurations.**
- ⊙ **Up to six distinct remanent bridge resistance levels.**

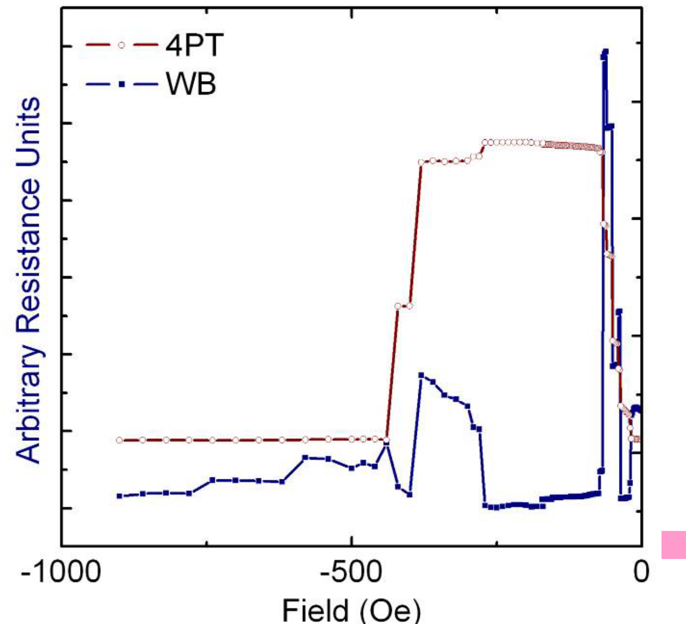

⊙ **Soft ring minor loops with Co layer in onion and vortex**

Wheatstone Bridge. NiFe/Cu/Co rings. Modeling

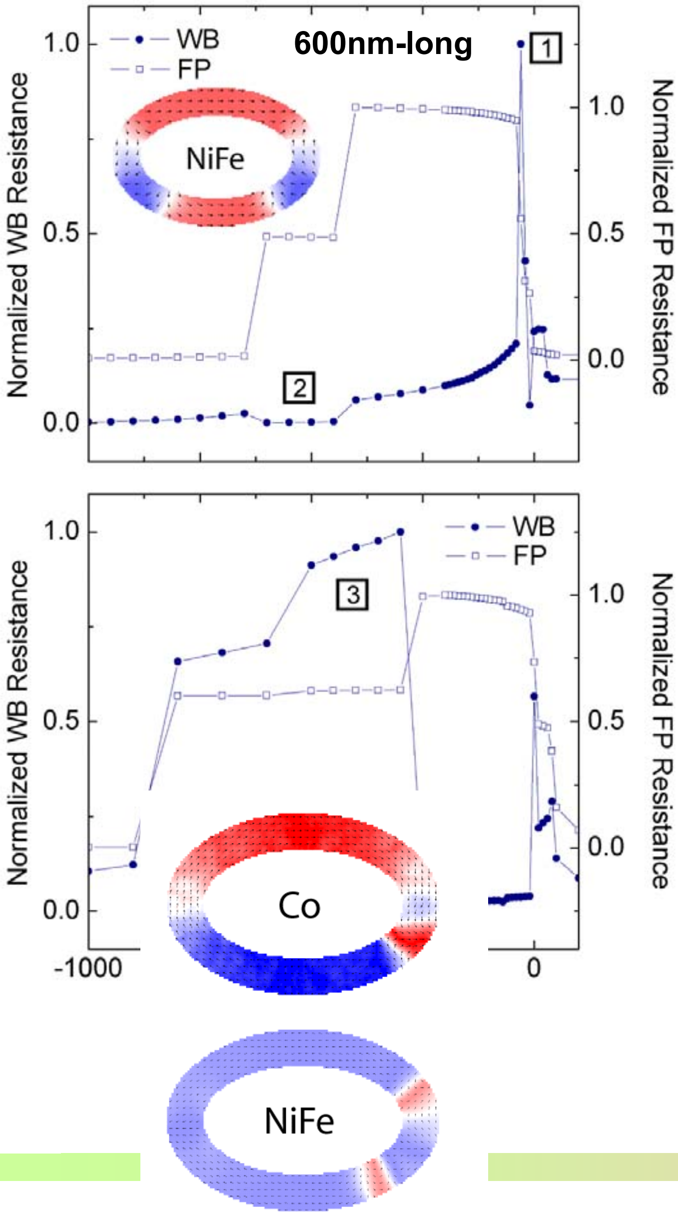

600nm-long

- **Computational analysis of micromagnetic modeling describes well magneto-transport response using both 4-point and Wheatstone bridge contact configurations.**

- **Wheatstone bridge measurements provide experimental evidence for**
  - **The soft ring reverses from both ends via four reverse domain walls.**
  - **360° domain walls can exit in the vortex configurations of multilayered rings.**

- **Similar magnetization reversal down to 150nm-long, 20nm-wide rings.**

Wheatstone Bridge measurements. Elliptical rings

- Soft layer reversal paths

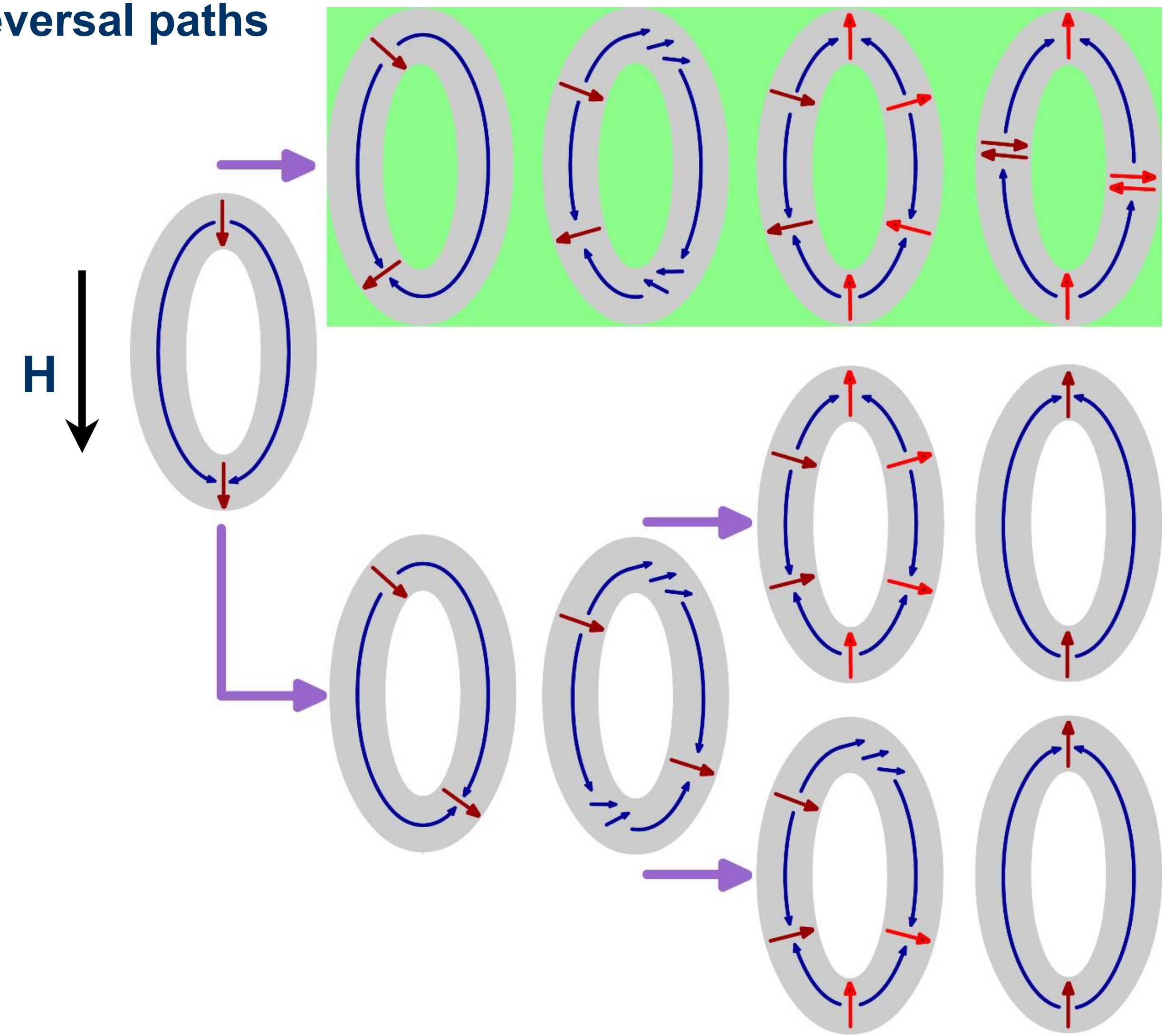

Elliptical rings. Soft ring phase diagram

- **Magnetic reversal not as simple as in single layers**
- **Soft layer**
  - **New reversal mechanism resulting from strong magnetostatic coupling due to the presence of domain walls in each of the rings**
  - **Reversal with 6 domain walls**

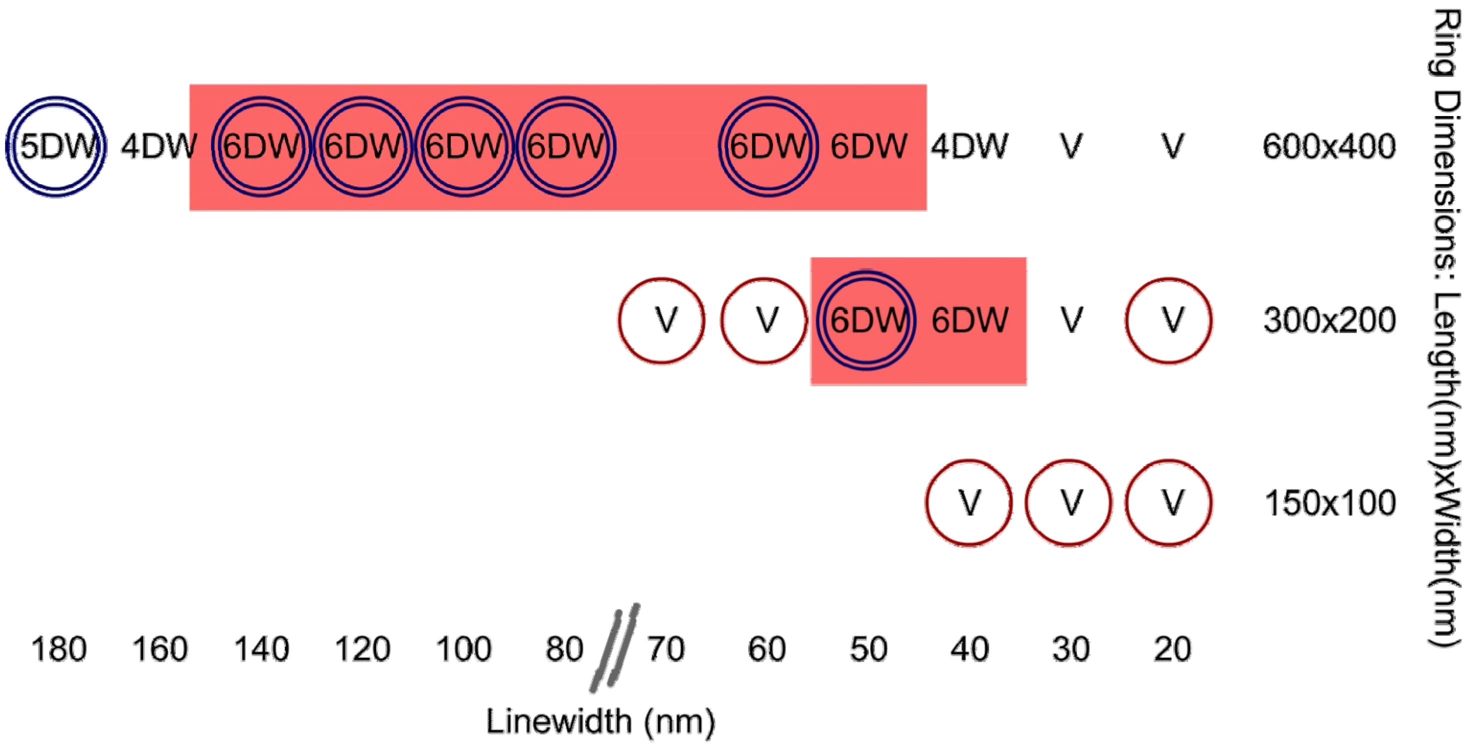

Rhombic rings. 4-point measurements

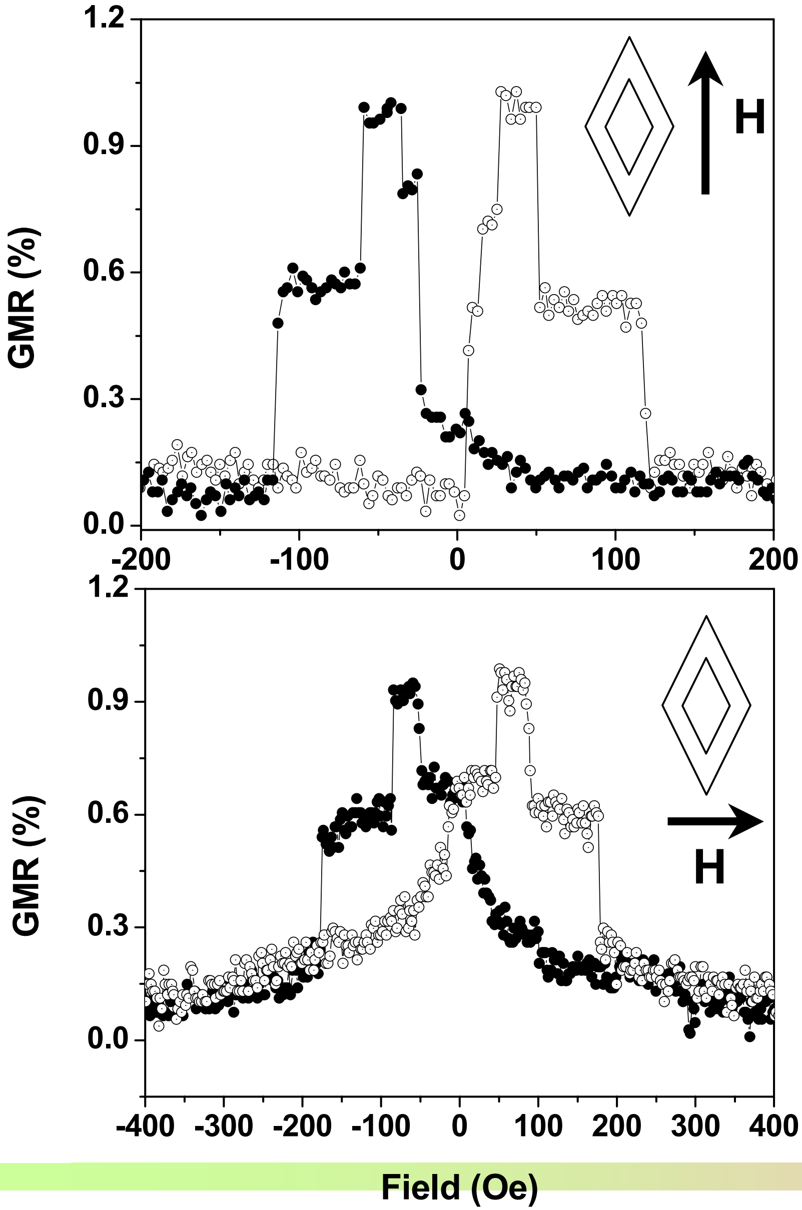

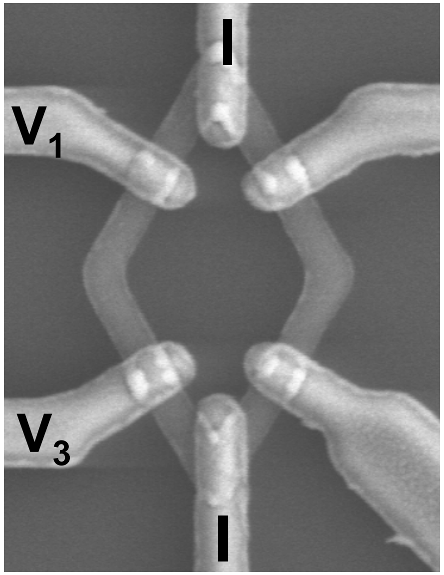

- ⊙ Measuring resistance using V_{13}/I.

- ⊙ Significantly lower switching fields for the soft and hard layers, compared with similar elliptical/circular rings.

- ⊙ Both layers reverse in fields below 200 Oe for both axis of the device.

Rhombic rings. Wheatstone bridge measurements

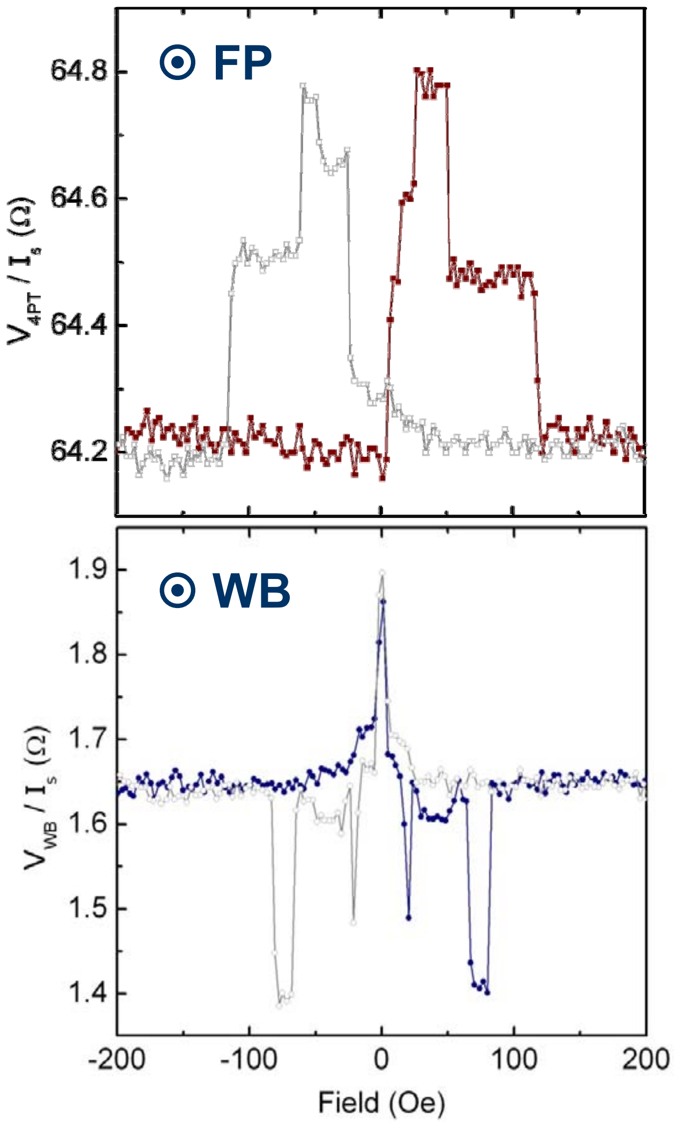

- ⊙ **WB is a true differential measurement**
- ⊙ **WB became unbalanced both as the soft ring reverses and as the hard ring switches into a vortex configuration**

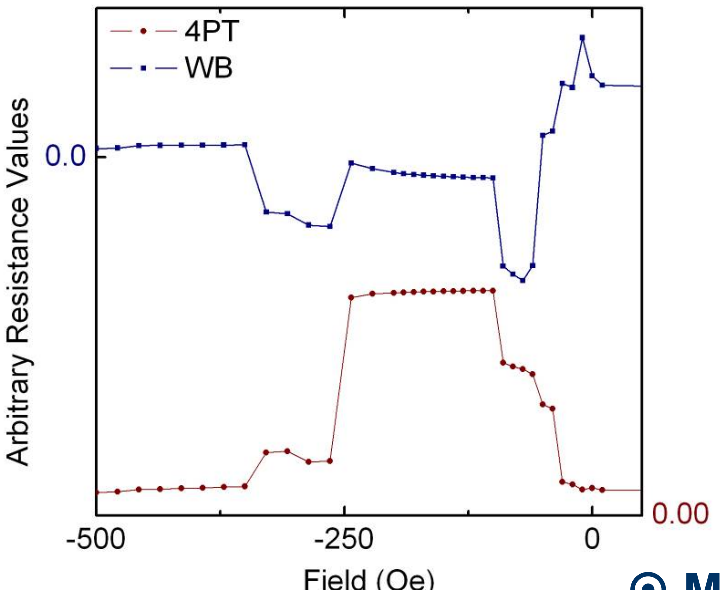

⊙ **Modeling**

Rhombic rings. Soft ring reversal

- Similar switching to elliptical multi-layered rings

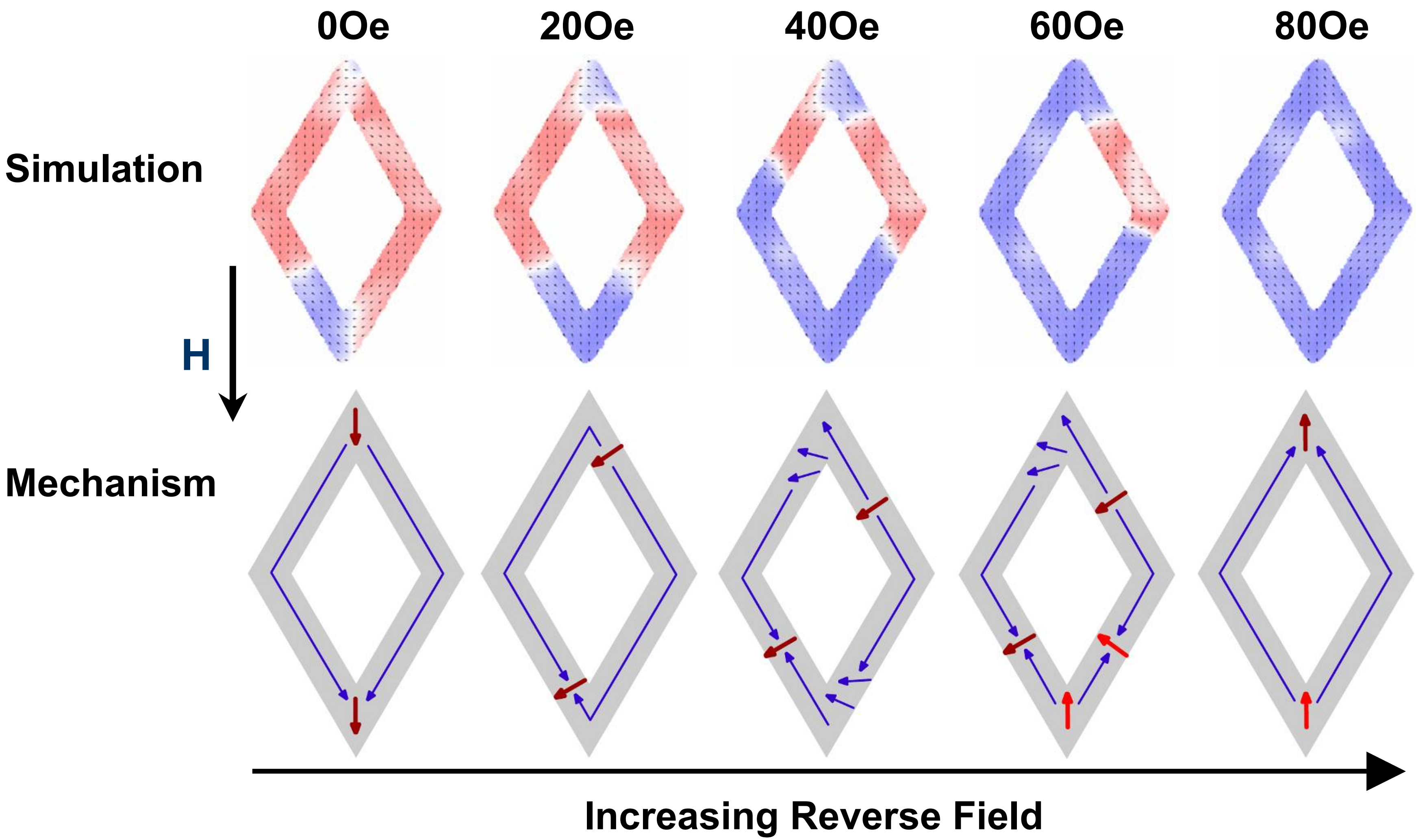

Rhombic rings. Hard ring reversal

- Formation of 4 reverse domains
- Much more controllable than elliptical rings

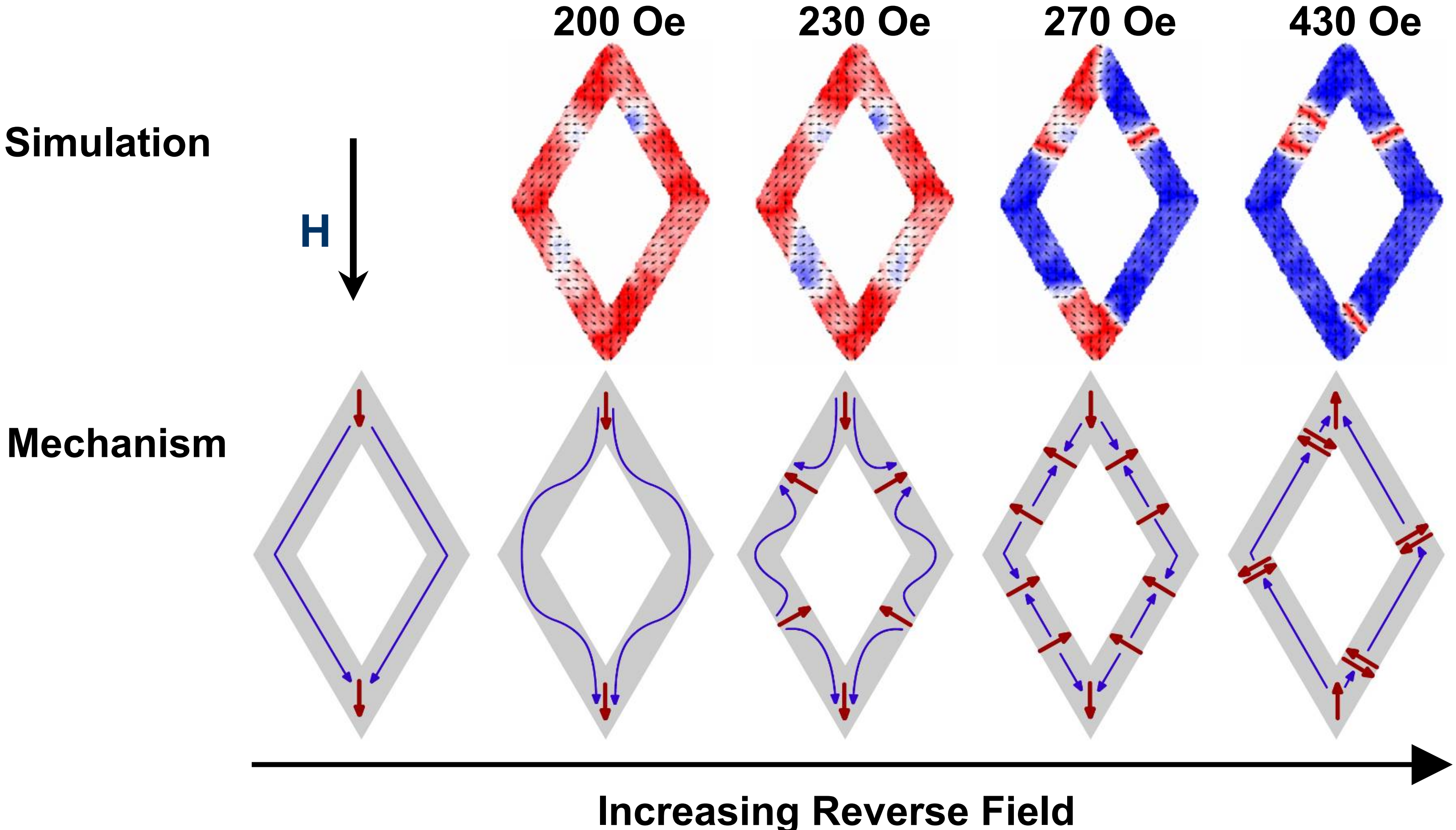

Rhombic rings. Hard ring reversal

- ⊙ Different symmetric behavior based on cycling from a saturated state (5000Oe) and an unsaturated (400Oe) state
- ⊙ Unsaturated cycling shows an intermediate state

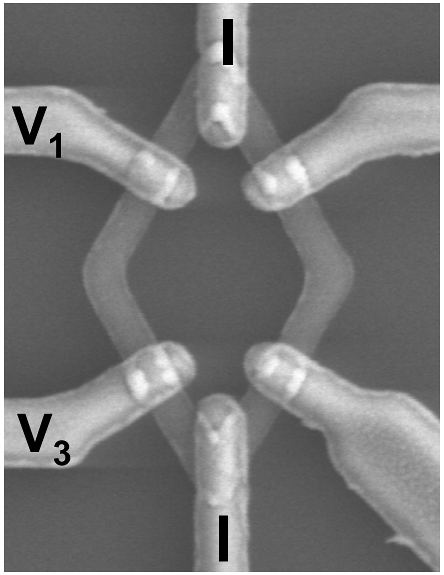

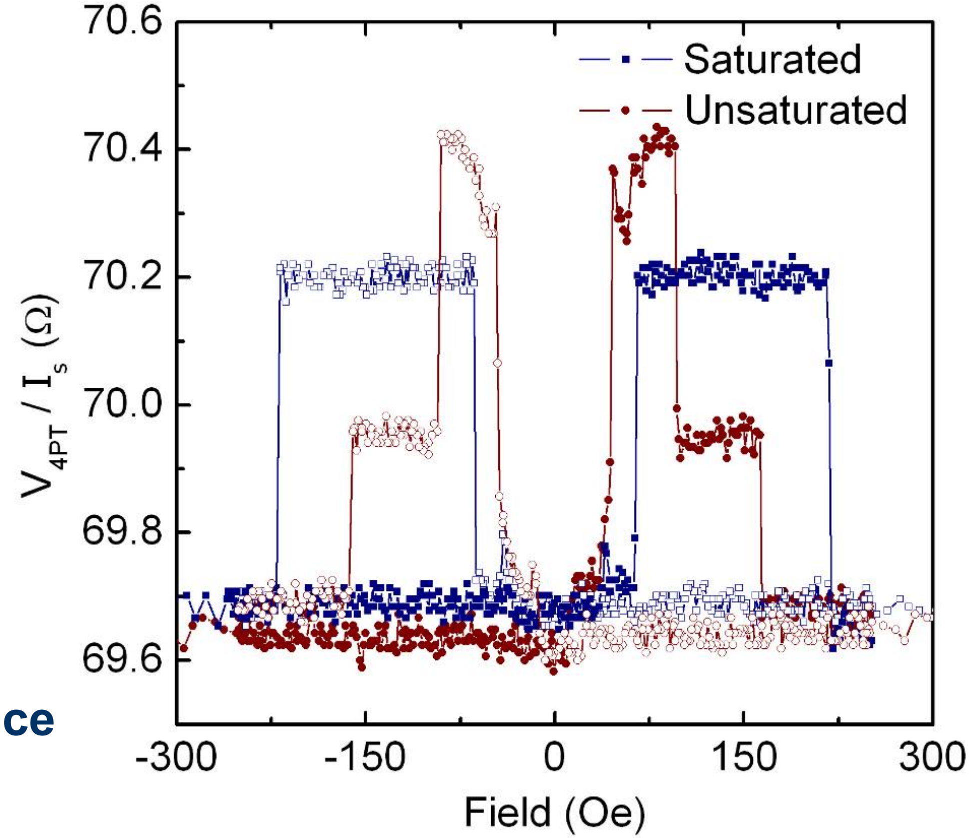

- ⊙ Evidence for the existence of stable 360° walls in the hard layer.

Current-induced switching. Multilayered rings

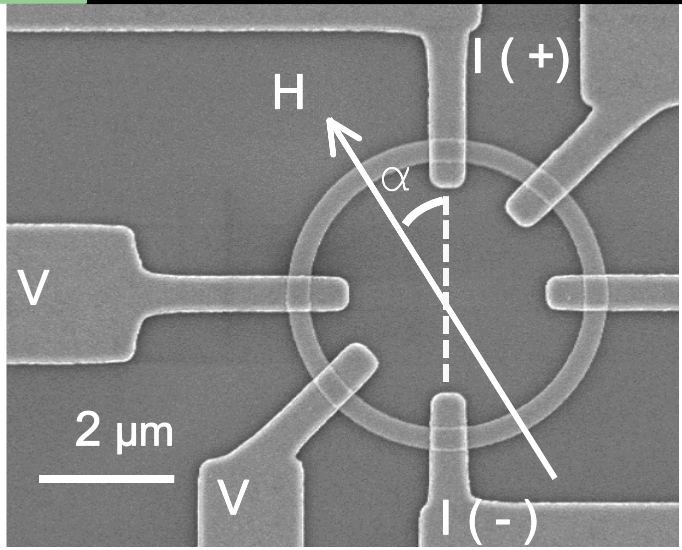

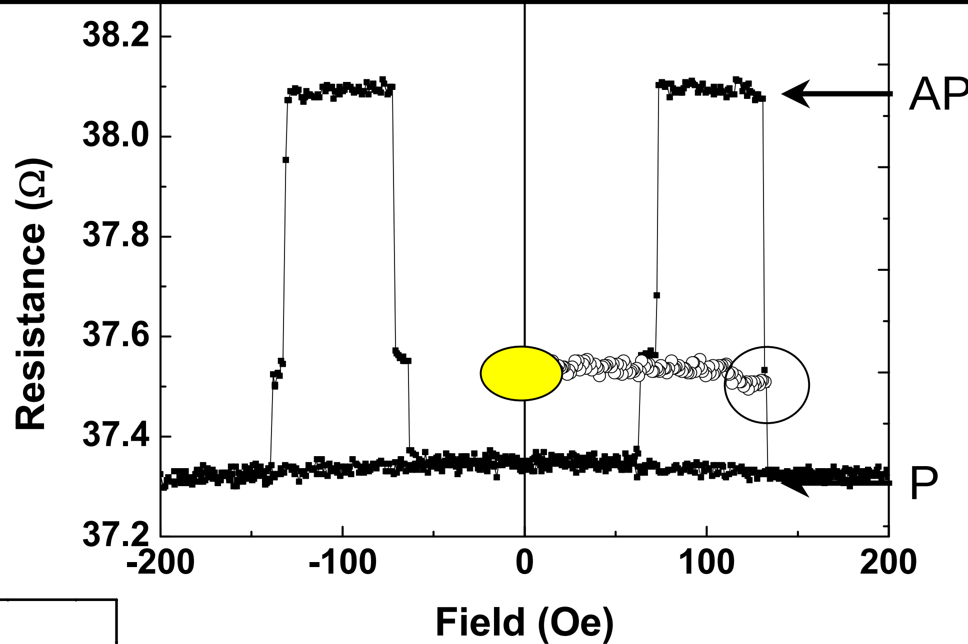

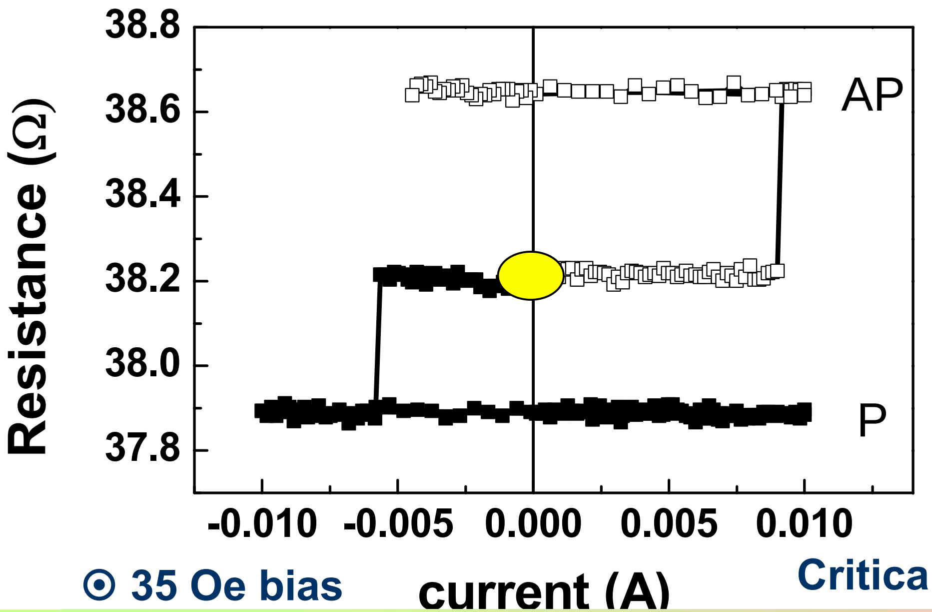

- Hard ring in vortex. CIMS of soft rings using 10µs-long pulses (0-10 mA)
- CIMS allows transitions from onion states to the desired vortex chirality by appropriate choice of current polarity.

- 35 Oe bias

Critical current densities ~ 3 x 10^7 A/cm^2

Current-induced switching. Multilayered rings

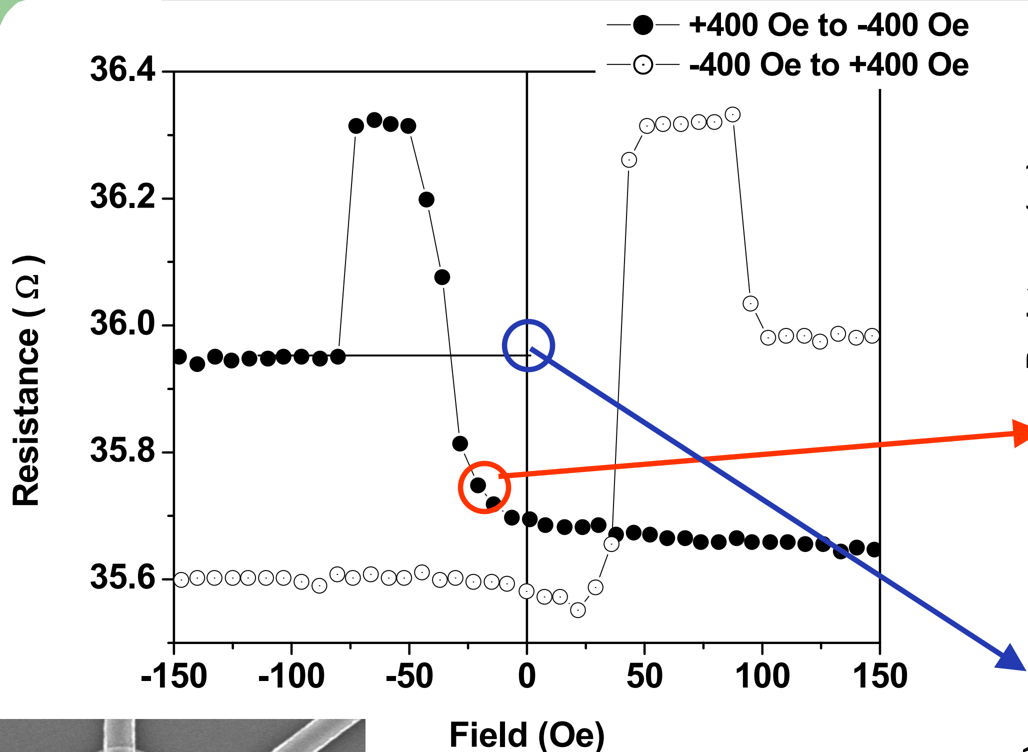

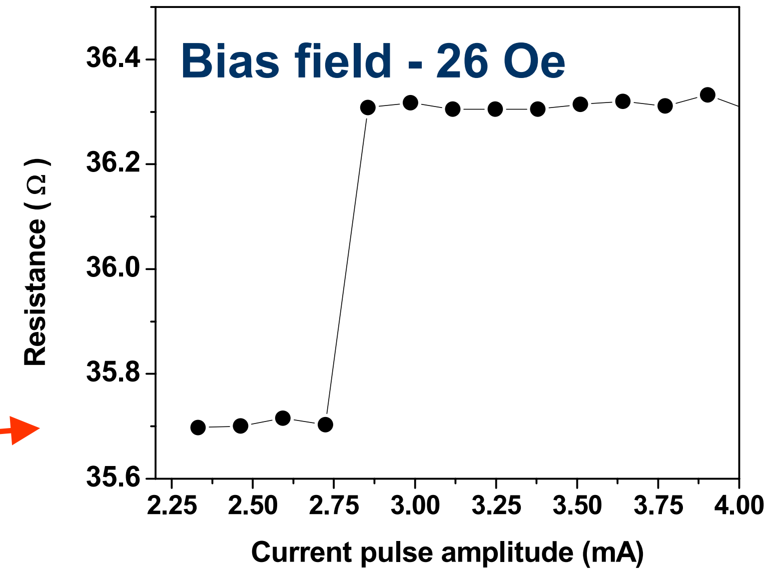

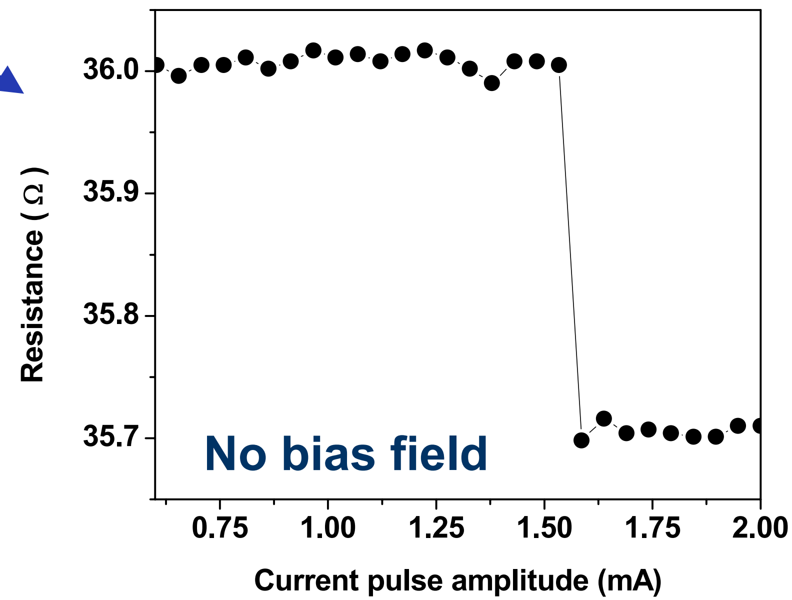

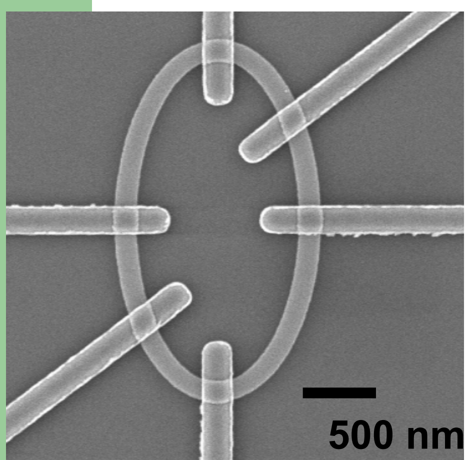

The same ring can be switched by a current pulse: with or without a bias field

Critical current density
3 x 10^7 A/cm^2

Device applications. Storage

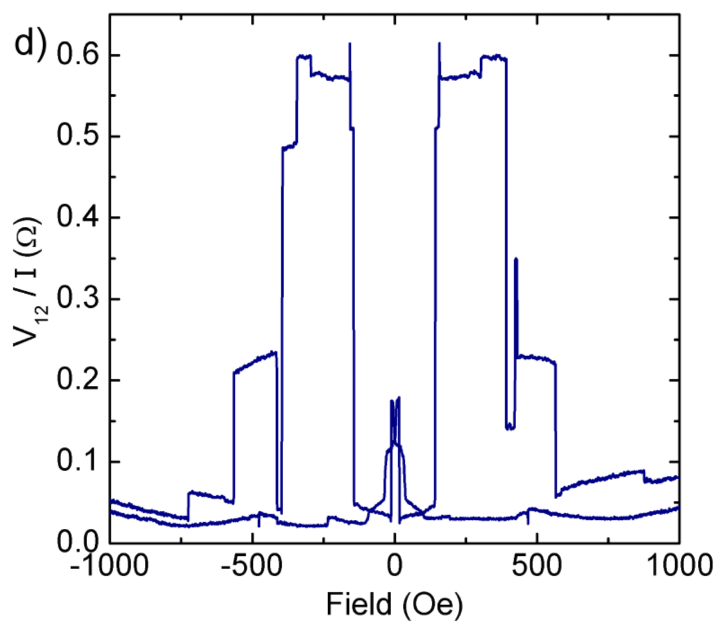

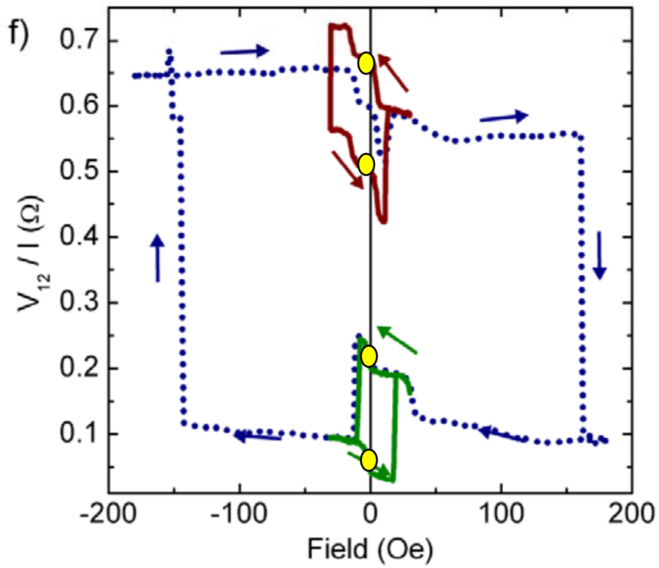

- **4-point measurements.**
  Different switching of the soft layer depending on the hard ring configurations. Interplay between shape anisotropy, contact arrangement and field direction. Up to 16 distinct remanece states for spin-valve rings

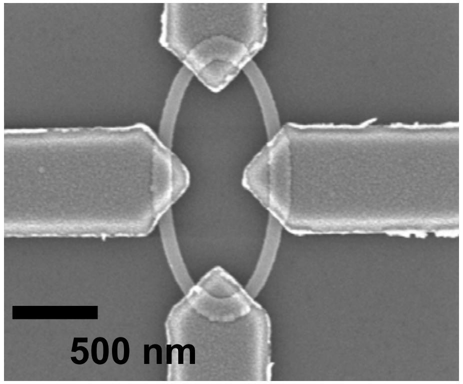

- **Wheatstone bridge**
  Unbalanced for vortex-like configurations in each ring. Lower switching fields.

1-bit storage

Cycling at fields of ±30 Oe

2-bit storage

Cycling at ±180 Oe, then ±30 Oe

Device applications. Logic

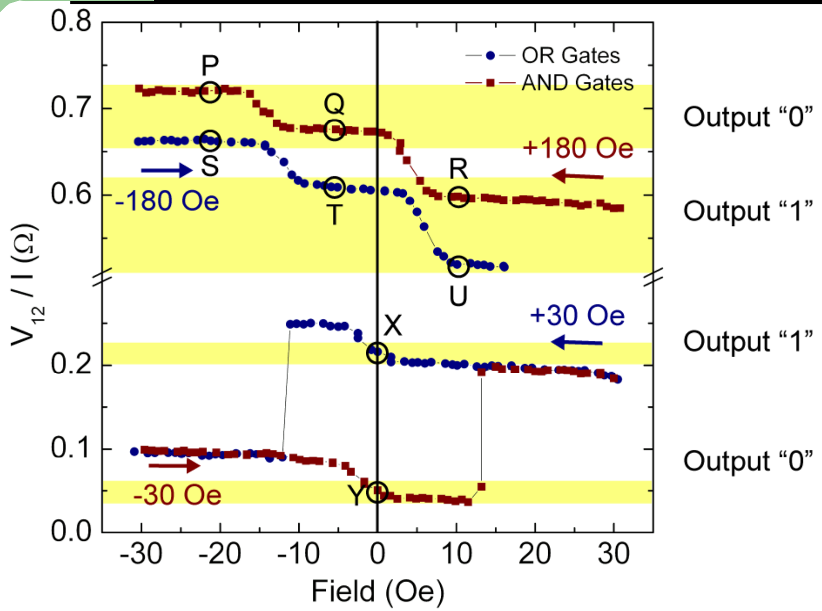

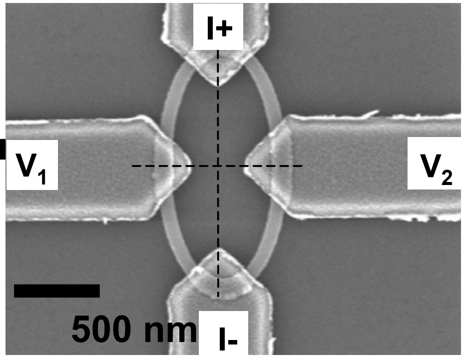

- **1st operation mode. Gate programming step, logic input step and logic read step.**

Ney et at, Nature 2003

Gate function needs to be reset using another ±30 Oe programming step

- **2st operation mode. Does not require reprogramming after each operation. Takes advantage of reversible, non-hysteretic movement of DW along the length of the ring at low fields**

Binary A	Binary B	Fields (Oe) A	Fields (Oe) B	Fields (Oe) A+B	+30 Oe OR		-30 Oe AND	
0	0	-15	-15	-30	0	Y	0	Y
0	1	-15	+15	0	1	X	0	Y
1	0	+15	-15	0	1	X	0	Y
1	1	+15	+15	+30	1	X	1	X

Binary A	Binary B	Fields (Oe) A	Fields (Oe) B	Fields (Oe) A+B	-180 Oe OR		+180 Oe AND	
0	0	-10	-10	-20	0	S	0	P
0	1	-10	+5	-5	1	T	0	Q
1	0	+5	-10	-5	1	T	0	Q
1	1	+5	+5	+10	1	U	1	R

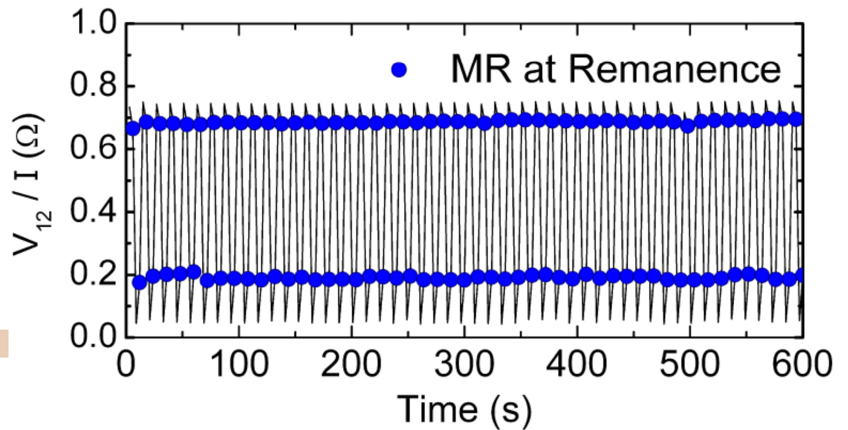

Summary

- NiFe/Cu/Co/Au and NiFe/Cu/Cu/IrMn/Au elliptical and rhombic rings display intermediate configurations on reversing both the soft (NiFe) and hard (Co) rings.
- These devices show a rich variety of stable and metastable magnetic states that can be accessed by field cycling at modest amplitude and/or by current-induced switching.
- Multiple remanent resistance levels and different switching behavior of the free layer depending on hard layer state.
  More than one-bit-per-cell in storage applications.
- Wheatstone bridge configurations allow additional insights on the magnetization reversal and provide for magneto-logic devices with improved functionality.